ISSN 0083-7903, 72 (Print)
ISSN 2538-1016; 72 (Online)

Oceanic Circulation and Hydrology off the Southern Half of South Island, New Zealand

by

R.A. HEATH

New Zealand Oceanographic Institute Memoir 72

1975

NEW ZEALAND

DEPARTMENT OF SCIENTIFIC AND INDUSTRIAL RESEARCH

Oceanic Circulation and Hydrology off the Southern Half of South Island, New Zealand

by

R.A. HEATH

New Zealand Oceanographic Institute, Wellington

New Zealand Oceanographic Institute Memoir 72

1975

Citation according to "World List of Scientific Periodicals" (4th edn)

Mem. N.Z. oceanogr. Inst. 72

ISSN 0083-7903

Received for publication : July 1972

A.R. SHEARER, GOVERNMENT PRINTER, WELLINGTON, NEW ZEALAND - 1975

CONTENTS

FIGURES

TABLES

Oceanic Circulation and Hydrology off the Southern Half of South Island, New Zealand

by

R.A. Heath

ABSTRACT

A survey of temperature and salinity variations with depth, conducted during February/ March 1970, is described for the region off the southern half of South Island, New Zealand.

Warm saline water of mainly subtropical origin was found to flow south-westwards down the west coast of South Island, eastwards across the Snares Shelf, and north-eastwards over the continental shelf off the east coast of South Island. Cooler, less saline, water flowed north-eastwards along the continental slope on the east coast of South Island towards the Mernoo Gap from where part flowed northwards through the Gap and the rest flowed eastwards along the southern flank of the Chatham Rise. Cool, low salinity, Subantarctic Water flowed generally in an eastwards direction over the Bounty Trough. An anticlockwise flow of Subantarctic Water (the Bounty-Campbell Gyral) was found in the south-western corner of the Bounty Trough.

INTRODUCTION

The oceanic flow off the bottom half of South Island, New Zealand, is in an anticlockwise direction. Previous studies have been made at fixed locations across the flow (e.g., Houtman 1966; Jillett 1969) but the continuity of the flow has hardly been studied. The present paper aims to discuss the spatial continuity of the flow in this area, by using both the geostrophic method and the changes in characteristics of the water along its flow path.

PREVIOUS WORK

The principal well-defined current in this region is the Southland Current. Garner's (1961) view of the Southland Current as a branch of the 'Tasman Current' which flows eastwards through Foveaux Strait into the surface water off the Otago coast was supported by Brodie (1960) who found that drift cards released on the west coast of South Island south of latitude 45°S were recovered on the east coast of South Island. Burling (1961) suggested that the Southland Current

New Zealand Oceanographic Institute Memoir 72. 1975. 36 pp.
ISSN 0083-7903

originated to the south-west of Stewart Island and consisted mainly of water from the Subtropical Convergence region, with some admixture of Australasian Subantarctic Water. Thus it appears that water which passes through a wide range of latitudes to the west of New Zealand can flow northwards in the Southland Current.

The circulation off the south-west coast of South Island has been shown by Garner (1967b) to be very complicated. A general inflow from the west had large vertical variations, with a south-going surface geostrophic flow relative to 500 dbar, and a north-going surface geostrophic flow relative to 1750 dbar.

The mainly subtropical nature of the Southland Current in Foveaux Strait has been confirmed by Houtman (1966). Jillett (1969) showed that off the Otago Peninsula the Southland Current was located on the continental shelf and slope, bounded on the seaward side by low salinity Subantarctic Surface Water.

Burling's (1961) analysis of the Southland Current System can be summarised as follows:- The Southland Front existed off the south-eastern coast of New Zealand as a subsurface feature in which the isotherms and isohalines sloped steeply downwards from the base of the summer thermocline (depth approximately 70 m) in the Subantarctic Water. This Front, which extended south to the Auckland Islands, marked the boundary between the Circumpolar Subantarctic Water and the warmer, more saline water of the Southland Current. South of the Subtropical Convergence in the Tasman Sea another front, the Australasian Subantarctic Front, was formed between Australasian Subantarctic Water (salinity >34.5‰) in the north, and Circumpolar Subantarctic Water (salinity <34.5‰) in the south, but this front was not dynamically connected with the Southland Front. The Australasian Subantarctic Water could not be recognised separately at the Southland Front since the waters of the Southland

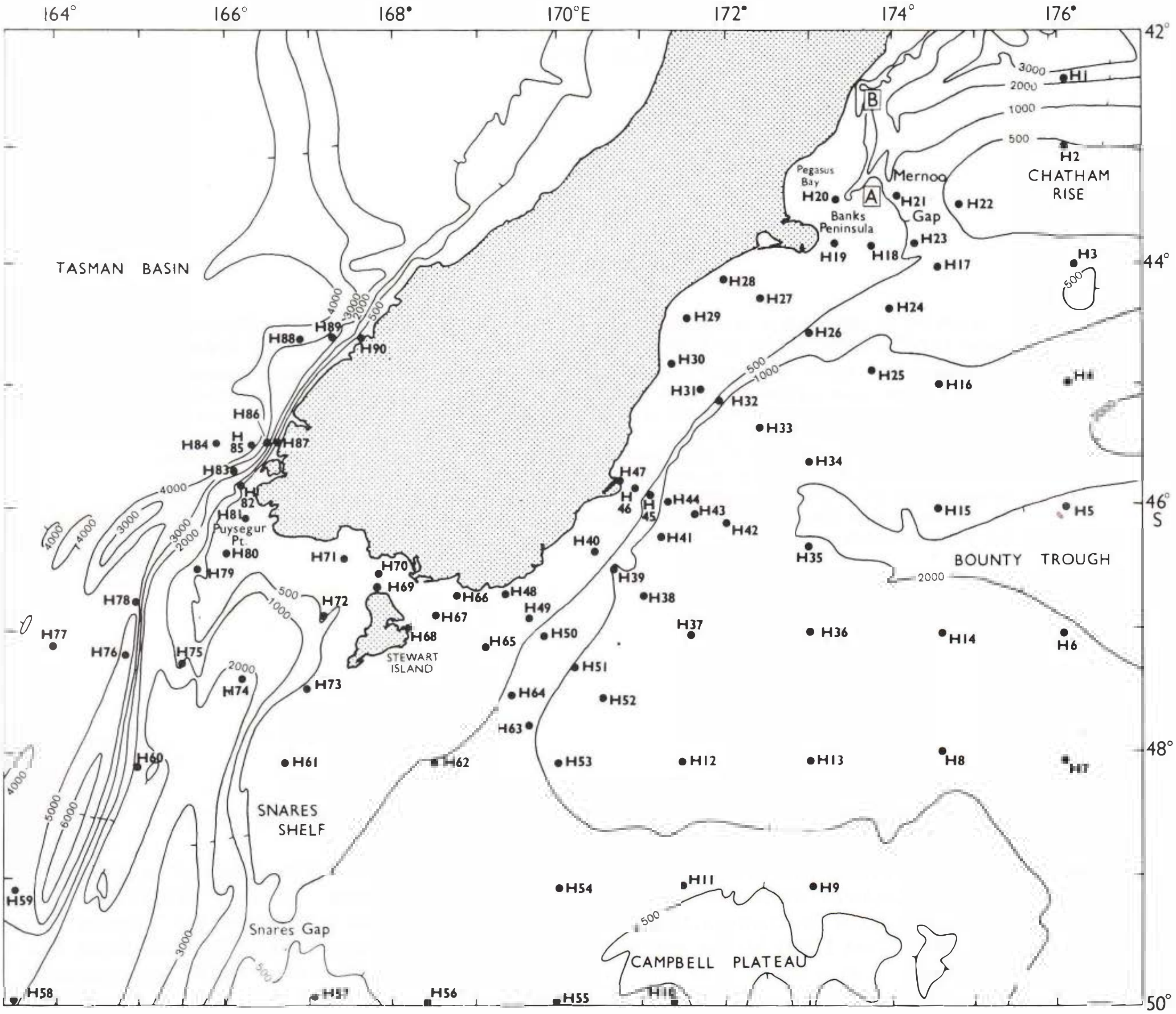

Fig. 1. Station positions for a cruise conducted between 3 February and 2 March 1970. The bathymetry of the survey area is also shown (in metres).

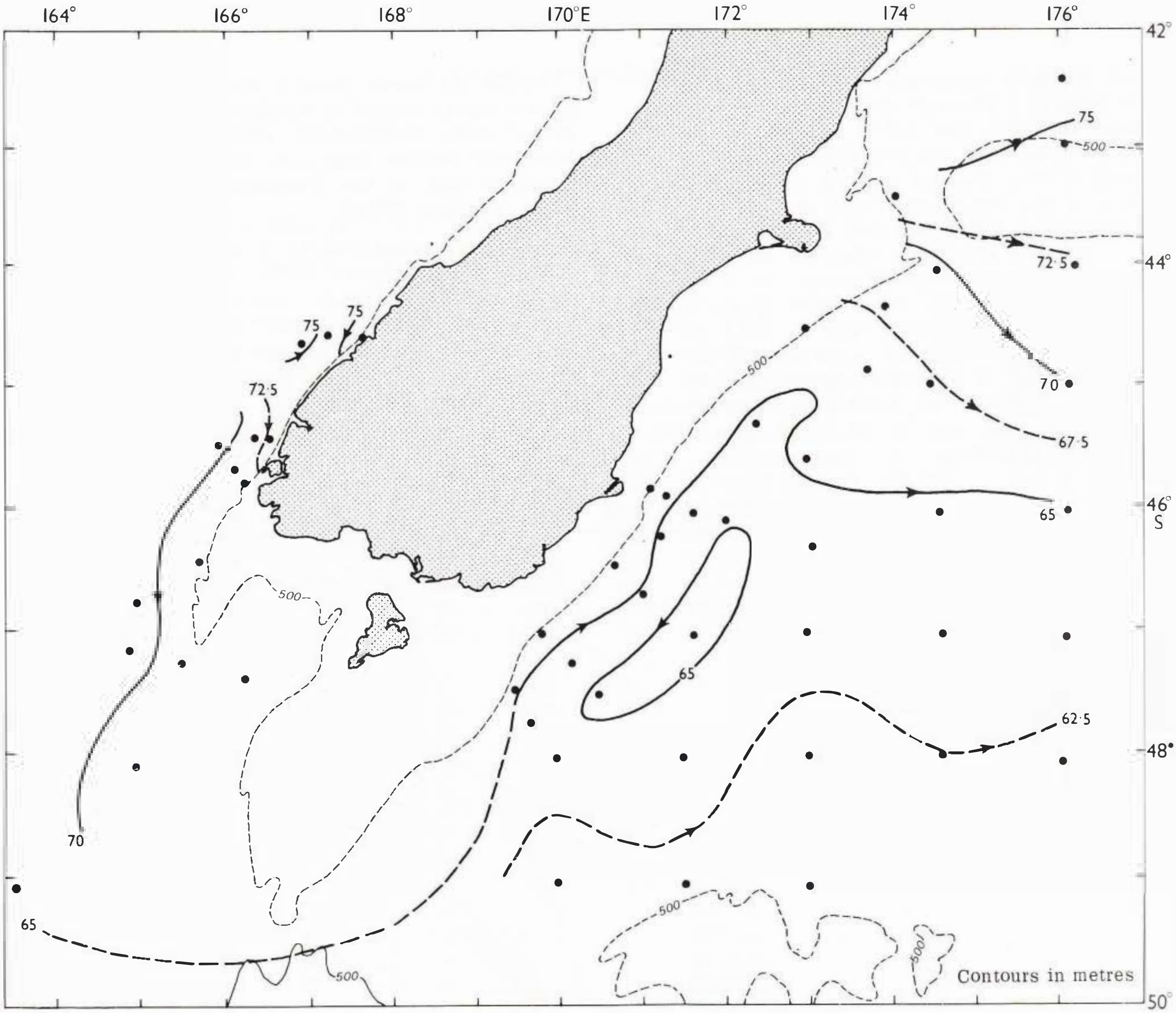

Fig. 2. Contours (dyn cm) of the geopotential topography of the sea surface relative to 500 dbar for data collected in February/March 1970. Arrows show flow direction.

Current were a mixture of both Subtropical and Australasian Subantarctic Water. At about 30-50 m depth, above the Southland Front, Circumpolar Subantarctic Water moved shorewards into the Southland Current and upwelled off Dunedin. Below 70 m the Southland Current continued mainly northwards until south of Banks Peninsula it turned eastwards. Above 70 m the water of the Southland Current mixed with the Circumpolar Subantarctic Water and continued mainly northwards along the east coast of South Island, as the "Canterbury Current"*.

* The term Canterbury Current has previously been used to define the northwards coastal flow to the north of Banks Peninsula. However, this flow has been shown to be continuous with the Southland Current, and it has therefore been suggested (Heath 1972b) that the term Canterbury Current is withdrawn and the term Southland Current used for all the northwards flow along the east coast of New Zealand.

Heath (1972a, b) showed that at least part of the subsurface water of the Southland Current passed northwards through a gap in the western end of the Chatham Rise (the Mernoo Gap, maximum depth 580 m) but the relative amounts of water passing northwards and eastwards still need to be examined.

Burling (1961) found the general movement in the western side of the Bounty Trough was counter-clockwise, the Bounty-Campbell Gyral, but as this interpretation was based on only a limited amount of synoptic data, it is open to question. Further east Heath (1968) found a general clockwise movement centred around latitude 45°30'S, longitude 178°E. Ridgway (pers. comm.) showed the surface geostrophic flow relative to 1000 dbar (calculated from data collected in January/February 1969 in the eastern side of the Bounty Trough) as being in a general clockwise direction centred at latitude 48°S, longitude 180°E.

OBSERVATIONS

Ninety standard temperature-salinity stations were occupied between 3 February and 2 March 1970, between longitudes 163°30'E and 176°E, and latitudes 50°S and 44°30'S to the west, and latitudes 50°S and 42°30'S to the east of New Zealand. Station positions and the bathymetry of the region are shown in Fig. 1; station circumstances are given in Table 1. This survey was the last in a series of summer block surveys conducted by the N.Z. Oceanographic Institute, to define the hydrology and circulation around New Zealand. The area discussed here is bounded by other block surveys. Garner (1967a) has described a survey off the east coast, to the north of the region discussed here, and also a survey (1967b) to the north on the west coast. A further survey to the east of the region was made in 1969 (Ridgway, in press).

Unlike the former surveys, where observations could in most cases extend to wirelengths of 2500 m, in this survey many observations were made in some comparatively shallow areas (i.e., the average depth of the surveyed part of the Campbell Plateau, the Snares Shelf, is about 300 m).

Data were collected in a manner similar to that described by Ridgway (1970). Station data and the derived water densities, cumulative dynamic height and potential energy anomalies are given in the Appendix. These measurements were supplemented by bathythermograph casts at each station and a continuous, sea surface, thermograph record.

Station sampling depths were restricted during several periods of gale-force winds.

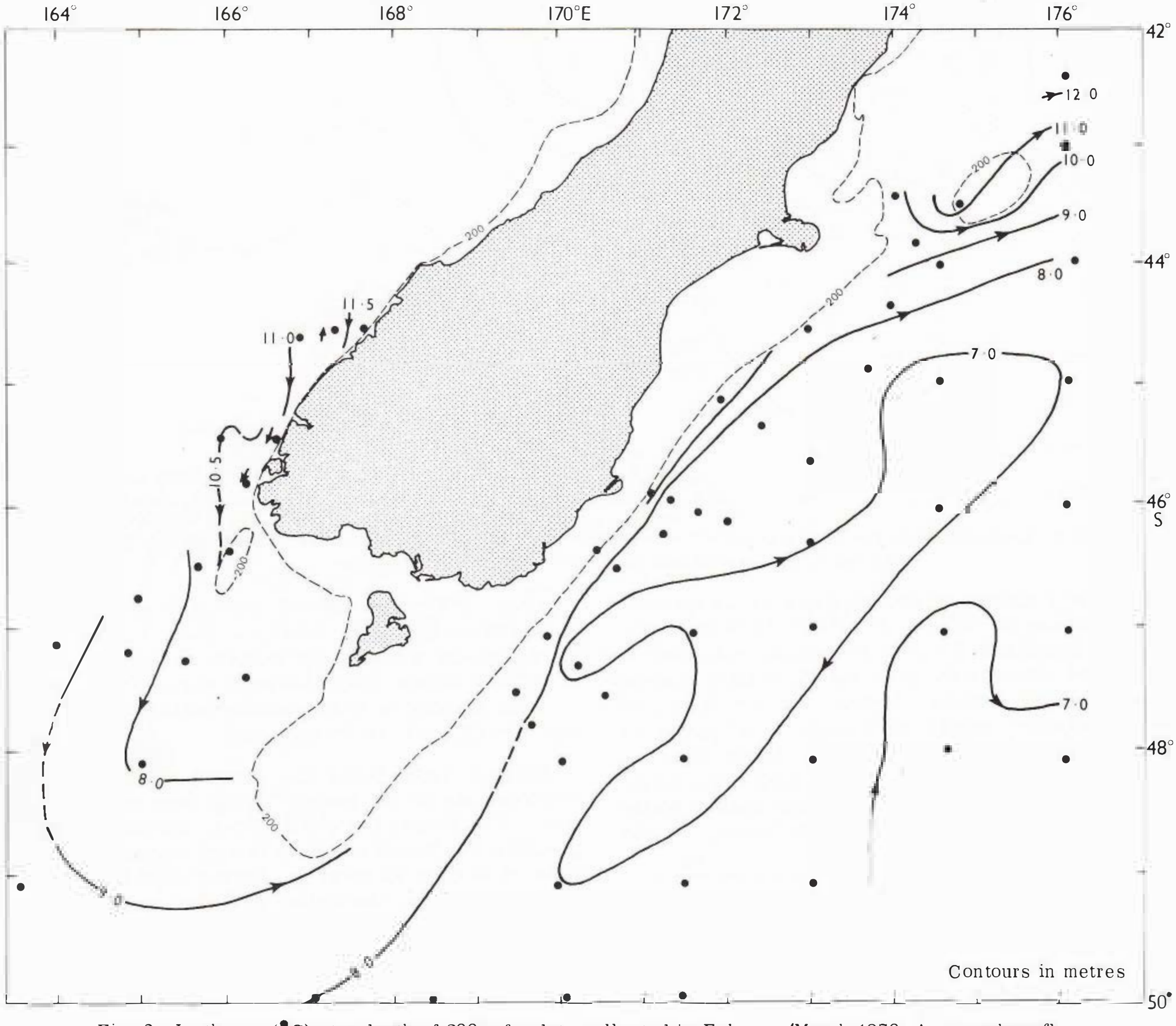

Fig. 3. Isotherms (°C) at a depth of 200 m for data collected in February/March 1970. Arrows show flow direction based on higher temperatures being on the left looking downstream.

TABLE 1

STATION CIRCUMSTANCES

Stn No.	Date Time N.Z. Start	Finish	Latitude (S) ° ′	Longitude (E) ° ′	Depth (m)
February 1970					
H1	3/1440	3/1628	42 25	176 00	1985
H2	3/2055	3/2210	43 00	176 00	530
H3	4/0652	4/0809	44 00	176 05.7	500
H4	4/1701	4/1835	44 58.7	176 03.2	1300
H5	5/0207	5/0638	46 00	176 00	2000
H6	5/1235	5/1418	47 00	175 59	1650
H7	5/2111	5/2248	48 00	176 00	1300
H8	7/0442	7/0625	47 55.5	174 30	1330
H9	7/1830	7/1952	49 00	173 00	595
H10	8/1014	8/1107	50 00	171 26.5	500
H11	8/1807	8/1905	49 00	171 30	560
H12	9/0137	9/0306	48 00	171 30	1300
H13	9/1008	9/1134	48 00	173 00	1200
H14	9/2105	9/2251	47 00	174 30	1320
H15	10/0630	10/0855	46 00	174 30	>1600
H16	10/1725	10/1841	45 00	174 30	1000
H17	11/0353	11/0532	44 00	174 30	520
H18	11/0938	11/1318	43 50	173 45	90
H19	11/1540	11/1622	43 50.2	173 15.5	72
H20	11/1906	11/1933	43 26.0	173 19.9	65
H21	11/2348	12/0115	43 24	174 04	710
H22	12/0523	12/0609	43 30	174 45	350
H23	12/0943	12/1145	43 51	174 15	450
H24	12/1516	12/1610	44 21	173 57.5	650
H25	12/1949	12/2131	44 52.5	173 44.5	1100
H26	13/0151	13/0248	44 32	173 00	560
H27	13/0657	13/0734	44 15	172 25	65
H28	13/0945	13/1013	44 05	172 00.5	22
H29	13/1330	13/1413	44 27.5	171 38.5	47
H30	13/2033	13/2117	44 48	171 22	33
H31	14/0036	14/0110	45 00	171 45	115
H32	14/0257	14/0654	45 04.0	171 55	520-400
H33	14/1005	14/1119	45 18.0	172 24.0	1420
H34	14/1538	14/1824	45 37	173 00	1500
H35	14/2225	14/2356	46 00	173 00	1500
H36	15/0722	15/0945	47 00	173 00	1300
H37	15/1709	15/1857	47 01	171 25.8	1320
H38	15/2305	16/0033	46 41	171 03	1100
H39	16/0325	16/0437	46 28	170 42	860
H40	16/0712	16/0806	46 19.7	170 29	140
H41	16/1231	16/1347	46 14	171 14	1185
H42	16/1755	16/1920	46 06.5	172 03	1370
H43	16/2132	16/2300	46 02.5	171 38.5	1400
H44	17/0054	17/0200	45 55.5	171 19	1080
H45	17/0605	17/0700	45 51.5	171 07.6	800
H46	17/0807	17/0828	45 49	170 56.4	102
H47	17/0938	17/0952	45 45.2	170 44.9	25
February 1970 continued					
H48	19/0553	19/0648	46 40.1	169 24.2	70
H49	19/0850	19/0925	46 52.5	169 40	117
H50	19/1042	19/1133	47 00	169 50	650
H51	19/1355	19/1520	47 15	170 10	1070
H52	19/1725	19/1938	47 30	170 29	1200
H53	19/2400	20/0148	48 00	170 00	900
H54	20/0830	20/0942	49 00	170 00	800
H55	20/1629	20/2112	50 00	170 00	600
H56	21/0507	21/0607	50 00	168 30	500
H57	21/1637	21/1929	50 00	167 02	150
H58	23/0515	23/0530	50 00	163 38.5	4750
H59	23/1743	23/2108	49 00	163 46.0	4300
H60	24/0633	24/0845	47 55	164 55	1800
H61	24/1643	24/1735	47 59.5	166 47	140
H62	25/0040	25/0139	48 00	168 30	130
H63	25/0736	25/0840	47 42	169 42	758
H64	25/1058	25/1145	47 27	169 29	480
H65	25/1429	25/1532	47 05	169 10	113
H66	25/1815	25/1848	46 45	168 53.1	55
H67	25/2022	25/2107	46 52	168 41.5	65
H68	25/2319	25/2400	46 57.5	168 20	50
H69	26/0442	26/0600	46 37.5	167 53.9	50
H70	26/0657	26/0728	46 30.1	167 52.6	43
H71	26/1032	26/1138	46 21	167 30	43
H72	26/1600	26/1656	46 47.5	167 19	138
H73	26/2330	27/0033	47 30	167 00	160
H74	27/0447	27/0723	47 18.7	166 05	1188
H75	27/1020	27/1202	47 13	165 13	823
H76	27/1516	27/1758	47 08	164 52	5500
H77	27/2208	28/0042	47 00	164 00	4400
H78	28/0615	28/0815	46 49	164 47.5	4650
H79	28/1320	28/1523	46 26	165 44	950
H80	28/1715	28/1754	46 22.8	166 01.6	185
H81	28/2036	28/2136	46 00	166 20	225
March 1970					
H82	28/2330	1/0155	45 46	166 09	1500
H83	1/0248	1/0619	45 39.5	166 09	2500
H84	1/0752	1/1041	45 22.2	166 00	4400
H85	1/1258	1/1512	45 24.5	166 22.5	3250
H86	1/1623	1/1824	45 24.8	166 33.9	2400
H87	1/1912	1/1942	45 24.8	166 42	150
H88	2/0145	2/0534	44 27	166 58	3600
H89	2/0727	2/0930	44 32.2	167 15	3600
H90	2/1133	2/1300	44 31.5	167 35.5	1000

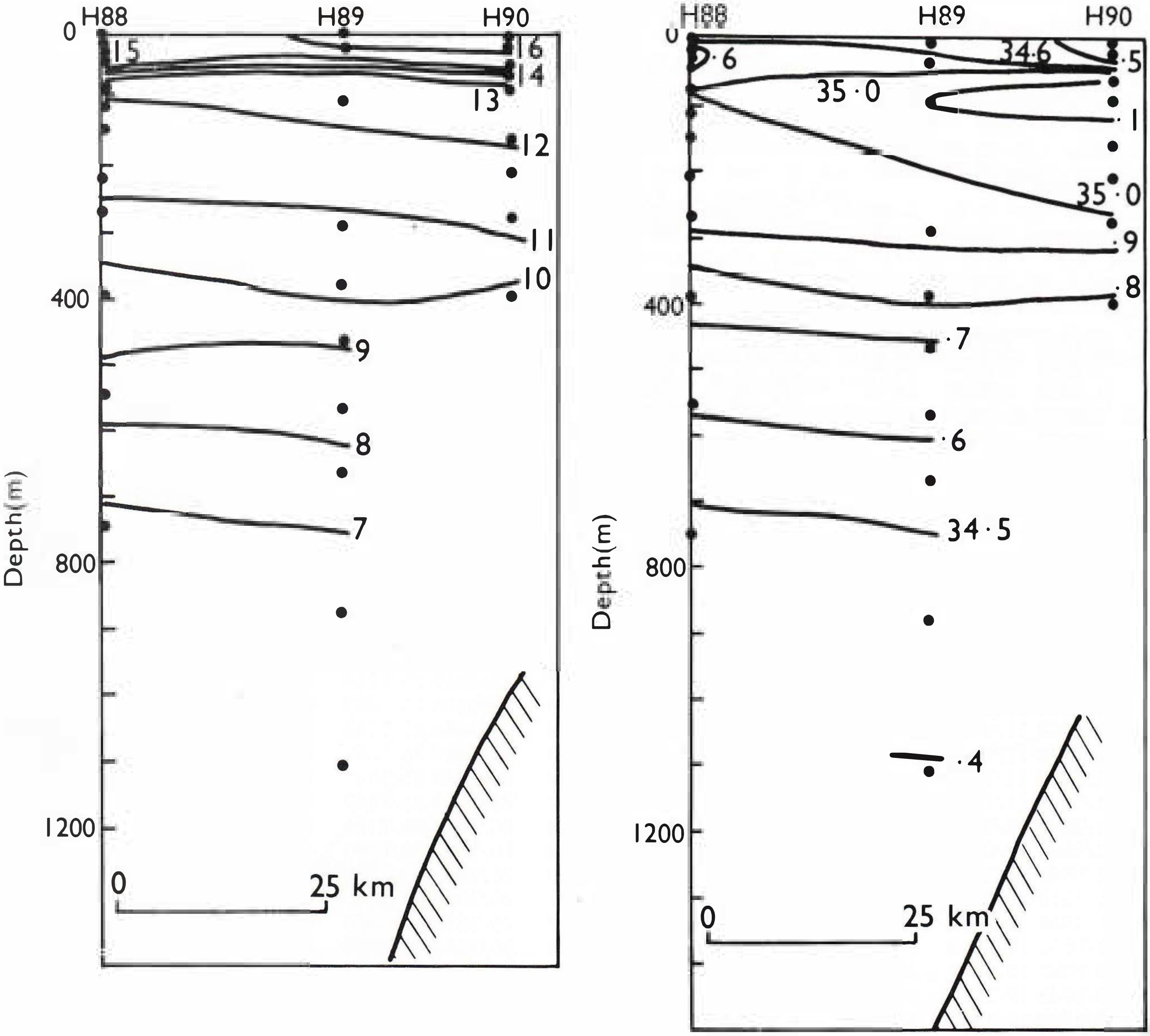

Fig. 4. Vertical cross-sections of temperature (°C) (left) and salinity (‰) (right) off the west coast of South Island, New Zealand.

DISCUSSION

GENERAL CIRCULATION

In the area surveyed the general direction of surface geostrophic current relative to 500 dbar (0/500 dbar) was from west to east, with the flow off the west coast of South Island being directed towards the south-west and that off the east coast being directed towards the north-east (Fig. 2). Close to the coast the distribution of temperature at 200 m (Fig. 3) was similar to the geostrophic circulation. Over the Bounty Trough where the relative geostrophic flow was weak (Fig. 2), there was less similarity between the two distributions (Figs 2, 3). The currents here were not constrained by topographic features as they were elsewhere in the surveyed area. Off the west coast, between stations H88 and H89, there was a weak flow towards the north.

Cross-section of temperature and salinity across the south-westwards flow off the west coast of South Island, and over the Macquarie Ridge, are shown in Figs 4-7. The southwards flow was intensified near the region of sloping bottom topography. Near-surface salinities were lowered by freshwater runoff from the Fiordland coast, Fiordland being a region of very high rainfall. The effect of runoff on the near-surface salinities in this area has previously been shown by Garner (1967b). Subsurface salinities, below the zone affected by coastal runoff, were largest close to the coast and decreased southwards (Figs 4-6). Deacon (1937) showed that, in the vertical plane, a subsurface tongue of high salinity water extended southwards from the Subtropical Convergence to, in places, almost the Antarctic Convergence. He explained its dynamics as follows:- "Whilst the wind drives the surface (subantarctic) water towards the north, another factor - the difference of climate between the southern and northern parts of the (subantarctic) zone - sets up a density gradient which tends to cause a current in the opposite direction". The subsurface salinitv maxima found at stations H59, 60, 75, 76, and 77 (Appendix) would result from this tongue, while closer inshore the development of a relatively high salinity subsurface water structure results from coastal dilution at the surface, the salinities being consistent with Subtropical Water flowing in from the north-west.

High salinity Subtropical Water flowed eastwards across the Snares Shelf and through the Snares Gap

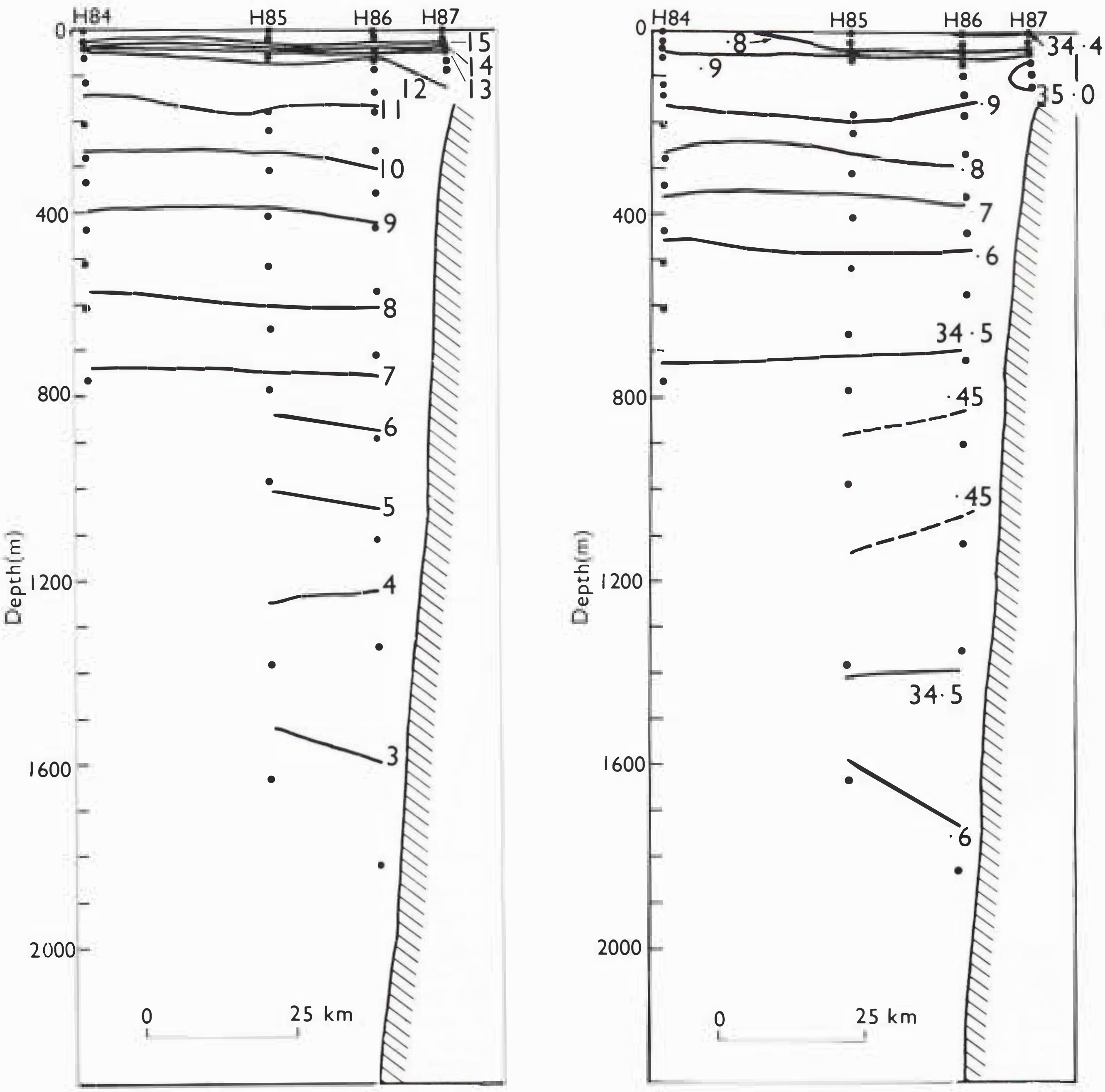

Fig. 5. Vertical cross-sections of temperature (°C) (left) and salinity (‰) (right) off the west coast of South Island, New Zealand.

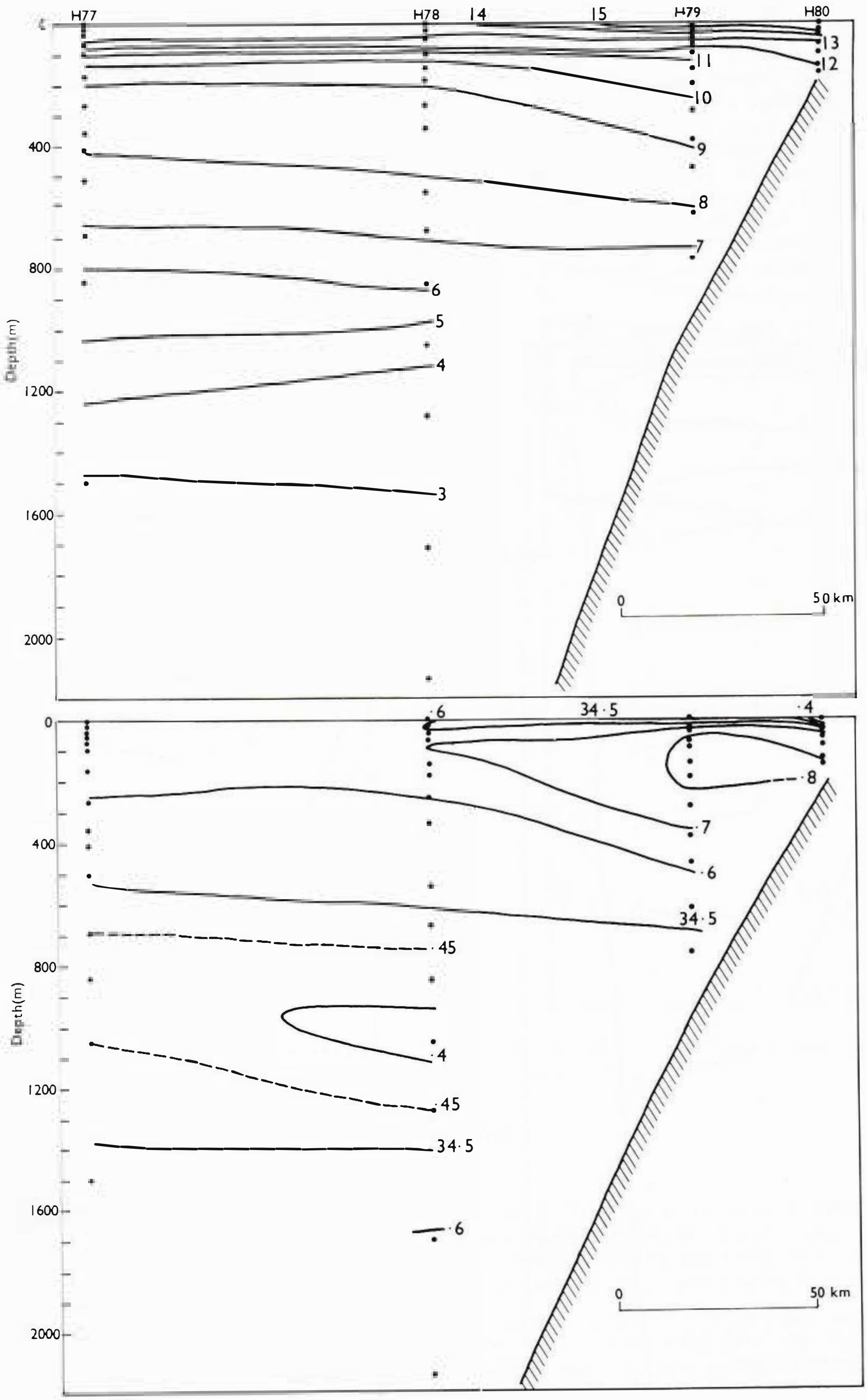

Fig. 6. Vertical cross-sections of temperature (°C) (upper) and salinity (‰) (lower) over the Macquarie Ridge. (Line joining Stns H77 to H80, Fig. 1.)

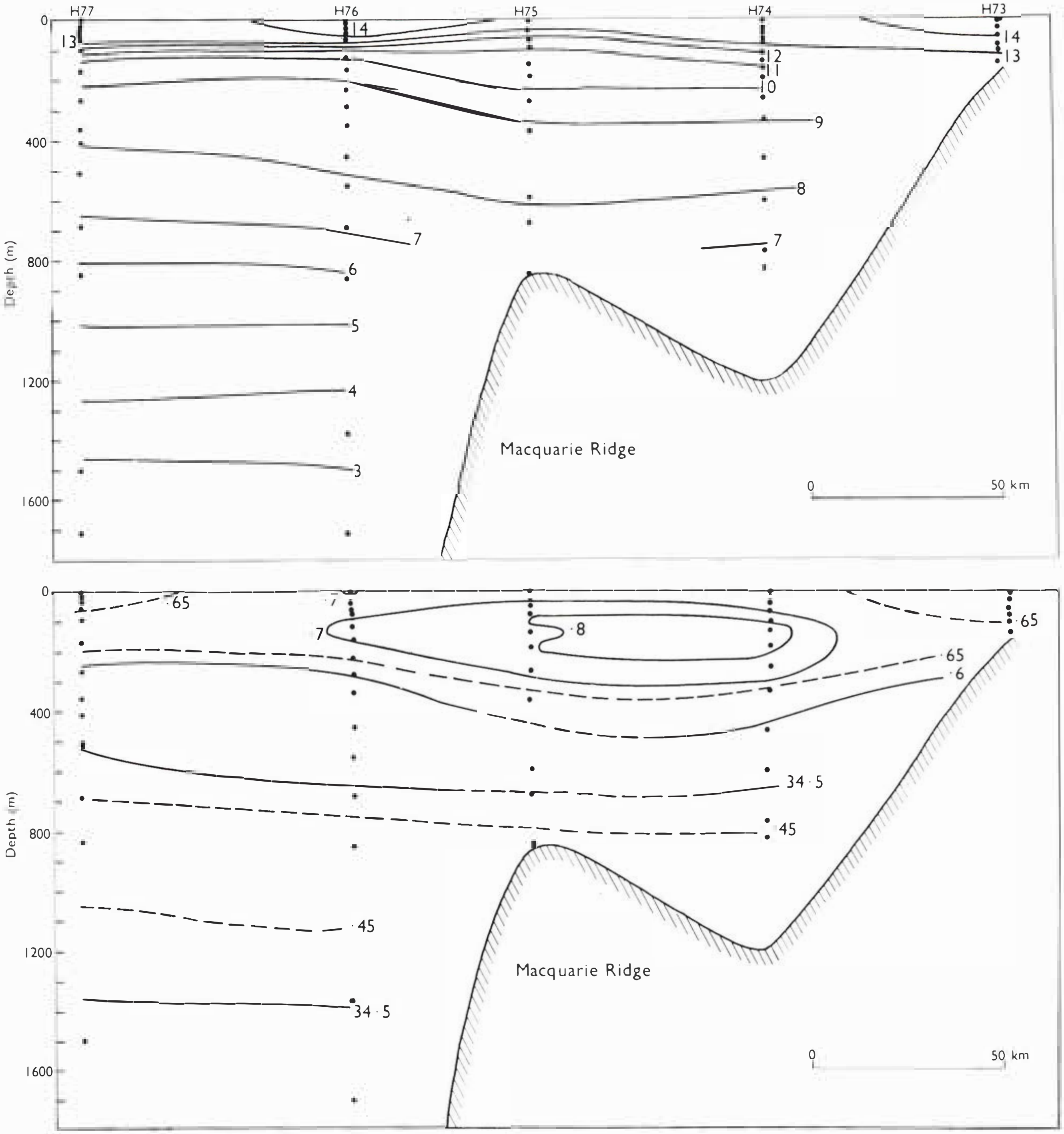

Fig. 7. Vertical cross-sections of temperature (°C) (upper) and salinity (‰) (lower) over the Macquarie Ridge. (Line joining Stns H77 to H73, Fig. 1.)

(Fig. 1), and turned north-eastwards off the east coast (Figs 2, 3, 14, 18-20). Cool, less saline water flowed along the continental slope of the Campbell Plateau (Figs 2, 7, 8) and also turned north-eastwards on the continental slope off the east coast. Thus, along the east coast, offshore from the region affected by coastal runoff, warm, saline Subtropical Water was found on the continental shelf and upper part of the continental slope (i.e., depths shallower than 200 m), overlaying low salinity, cooler water of Subantarctic origin. The region of relatively high horizontal gradients of salinity and temperature between the Subtropical Water inshore and the Subantarctic Water offshore is the Southland Front (Figs 8-13). The Front is formed as a gradual rather than an abrupt change in hydrological properties, and is therefore best regarded as a zone of finite horizontal and vertical extent rather than a planar boundary. Burling (1961) found that this Front arises

Sig. 3

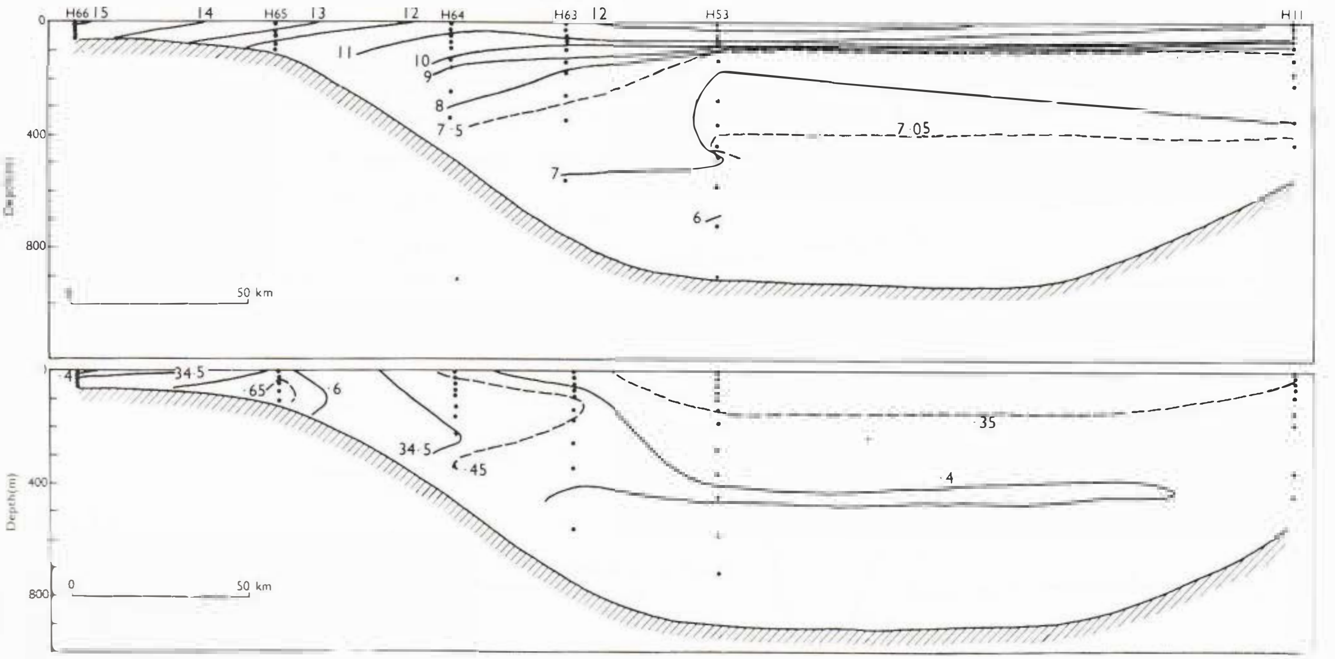

Fig. 8. Vertical cross-sections of temperature (°C) (upper) and salinity (‰) (lower) off the east coast of South Island, New Zealand. (Line joining Stns H11 to H66, Fig. 1.)

at its southern extremity as the boundary where oppositely directed flows of Subantarctic Water meet but, off the east coast, the contrast is accentuated by the presence of Subtropical Water on the continental shelf. Because all the water in the Southland Front, as well as that closer inshore, travels northwards off the east coast, this entire flow should be referred to as the Southland Current and not just "the flow of Subtropical Water".

FLOW NEAR THE CHATHAM RISE

Burling (1961) showed the Southland Front as extending northwards past Dunedin, then eastwards south of Banks Peninsula to become continuous with the Subtropical Convergence over the Chatham Rise. He stated that below 75 m the Southland Current was deflected to the east, south of Banks Peninsula. However, Heath (1972a, b) found that the Southland Front extended northwards through the Mernoo Gap, with cool, low salinity water being forced upwards through the Gap so that the Southland Current was recognised as a low salinity, low temperature, tongue of water north of the Mernoo Gap. The western side of this tongue was the Southland Front and the eastern side the northward extension of the Subtropical Convergence. In the present survey, cool, low salinity water of Subantarctic origin was found over the continental slope forming the western side of the Mernoo Gap (*see* Stns H21, 23, 26 *in* Fig. 15) and also north of the gap, and warmer, more saline water of mixed Subantarctic and Subtropical origin was found over the eastern side of the Gap. Low salinity water was also found at Stn H3 (Figs 15, 17) located east of the Mernoo Gap, on the southern flank of the Chatham Rise (Figs 16, 17) and, because the flow near this station was towards the east (Fig. 2), low salinity water must have flowed from the vicinity of the southern entrance to the Mernoo Gap. Therefore, it can be seen that water of Subantarctic origin flows both northwards through the western side of the Mernoo Gap and eastwards along the southern flank of the Chatham Rise. The form of the isolines at the Subtropical Convergence over the Chatham Rise (Figs 16, 17) is similar to those at the Southland Front on the continental slope south of the Mernoo Gap. However, these two regions of rapid spatial change of water properties are not continuous, since they are separated by the presence of low salinity water in the Mernoo Gap. For this reason it is probably better to confine (a) the term Southland Front to that portion of the boundary between the warm, saline inshore water and the cooler, less saline offshore water on the continental slope, and (b) the term Subtropical Convergence to the region where the warm, saline Subtropical Water meets the cool, less saline Subantarctic Water along the Chatham Rise and in the Southland Current north of the Chatham Rise (*see* Heath 1972a, b; in press).

Direct Current Measurements

The relative amounts of water passing northwards through the Mernoo Gap, and eastwards along the southern flank of the Chatham Rise can be determined only by direct current measurements. Heath (in press) has shown that anticyclonic eddies of Subtropical Water are shed from a larger eddy situated at approximately latitude 41°30'S, longitude 178°E. These eddies are guided by the bottom topography towards either Kaikoura or the northern end of the Mernoo Gap.

Because the transport of the Southland Current will be greatly affected by the presence or absence of one of these eddies, the relative transports of water southwards and eastwards from south of the Mernoo Gap must be highly variable. Direct current measurements were recently made both in the Mernoo Gap and near Kaikoura, using parachute drogues (Heath 1973). On 23 April 1970 a drogue was launched in the northern end of the Mernoo Gap at position latitude 43°26'S, longitude 173°48.6'E (position A, Fig. 1, bottom depth 360 m), and over a 9.8 h period the mean current velocity at a wire length of 300 m was 8.5 cm s^{-1} towards 025°T. Near the same launching position the mean current at a wire length of 100 m was 26 cm s^{-1} at 049°T over 6.5 h. Both of these measurements had a marked tidal effect, the drogues initially moving slowly southwards. Near Kaikoura (latitude 42°36'S, longitude 173°45'E) (position B, Fig. 1, bottom depth 850 m) the drogue at a wire length of 500 m had a mean speed of 19 cm s^{-1} at 029°T over 7 h, and at a wire length of 100 m had a mean speed of 21 cm s^{-1} towards 026°T over 10.5 h. Tidal effects on both of these measurements were marked by changes in speed but not in direction. (For an extended analysis of these current measurements *see* Heath (1973).) These four current measurements confirmed the presence of a relatively strong northwards flow along the continental slope northwards from the Mernoo Gap, which must be fed from the northwards flow which passes along the continental slope and through the western side of the Mernoo Gap.

North of the Chatham Rise the geostrophic flow in the Subtropical Water was towards the east (Fig. 2); this agrees with previous geostrophic circulation patterns in this area (Garner 1967a; Heath 1968, 1972b, 1973).

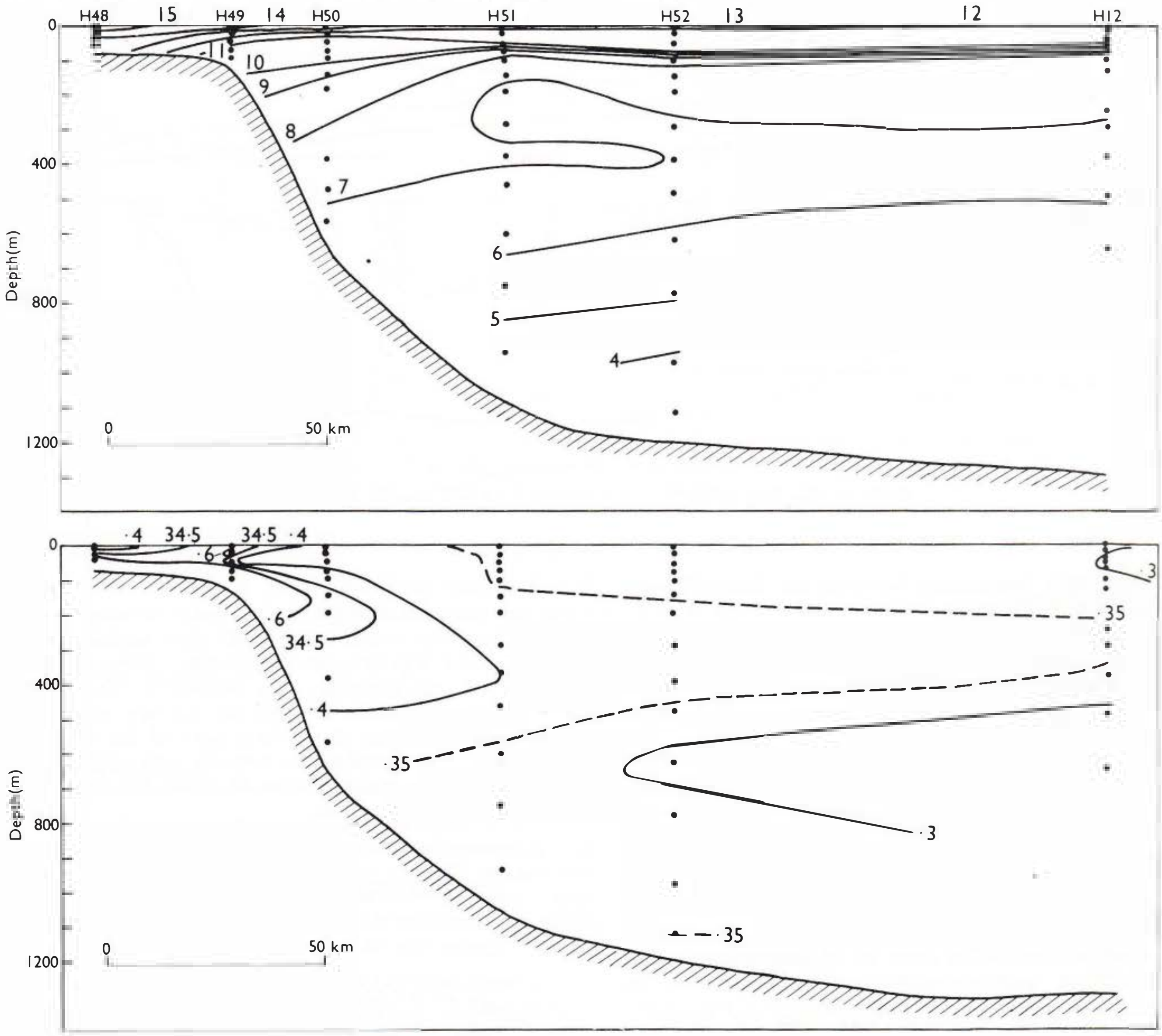

Fig. 9. Vertical cross-sections of temperature (°C) (upper) and salinity (‰) (lower) off the east coast of South Island, New Zealand. (Line joining Stns H12 to H48, Fig. 1.)

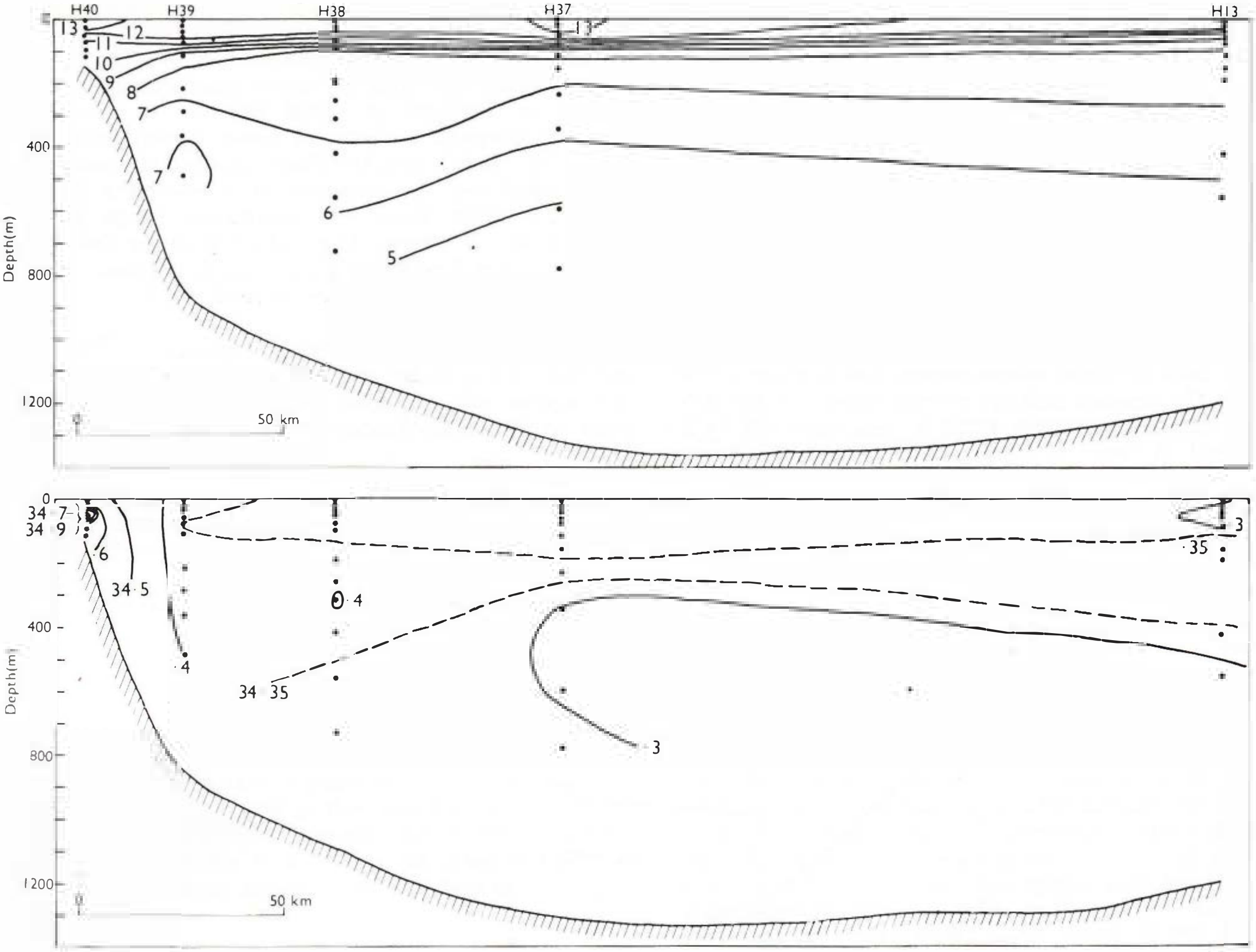

Fig. 10. Vertical cross-sections of temperature (°C) (upper) and salinity (‰) (lower) off the east coast of South Island, New Zealand. (Line joining Stns H13 to H40, Fig. 1.)

FLOW OVER THE BOUNTY TROUGH

The relative geostrophic flow over the Bounty Trough was much weaker than in the Southland Current (Figs 2, 10-12). Burling (1961) postulated the presence of an anticyclonic rotation, the Bounty-Campbell Gyral, in the western side of the Bounty Trough (*see* Burling 1961, chart 1). Heath (1968) found that the geostrophic currents of the surface relative to 1000 dbar near position 45°30'S, 178°E were in a general clockwise direction, with a maximum speed of 8.8 cm s^{-1}. Ridgway (pers. comm.) found a strong clockwise movement in the surface geostrophic current relative to 1000 dbars centred about 49°S, 180°E. In the present study surface geostrophic currents relative to 500 dbar (Fig. 2) showed a weak anticlockwise movement near position 47°S, 171°E, immersed in a general flow eastward over the Bounty Trough. The position of the centre of this anticlockwise movement agreed with that given by Burling (1961) for the Bounty-Campbell Gyral. Integrating all previous current observations over the Bounty Trough (Burling 1961; Heath 1968; Ridgway, pers. comm.) with those given here the general circulation consists of -

1. A strong northwards flow of Subantarctic Water along the continental slope, and of water of subtropical origin along the continental shelf (the surface geostrophic speed with respect to 500 dbar between Stns H44 and 45, off Dunedin, was 20 cm s^{-1}). The shelf water flows northwards through the eastern side and inshore of the Mernoo Gap, while part of the Subantarctic Water flows through the western side of the Gap and the remainder flows eastwards along the southern flank of the Chatham Rise.

2. A general weak movement from west to east over the Bounty Trough (surface geostrophic speed 0/500 dbar 1-6 cm s^{-1}) is met by a strong northwards flow along the Subantarctic Slope to the east of the Bounty Islands, giving rise to a strong clockwise flow.

3. A weak anticlockwise flow about 50-100 km across centred near 47°S, 171°E, lying between the northwards flowing Southland Current to the east of Stewart Island and the general east-west flow, the Bounty-Campbell Gyral.

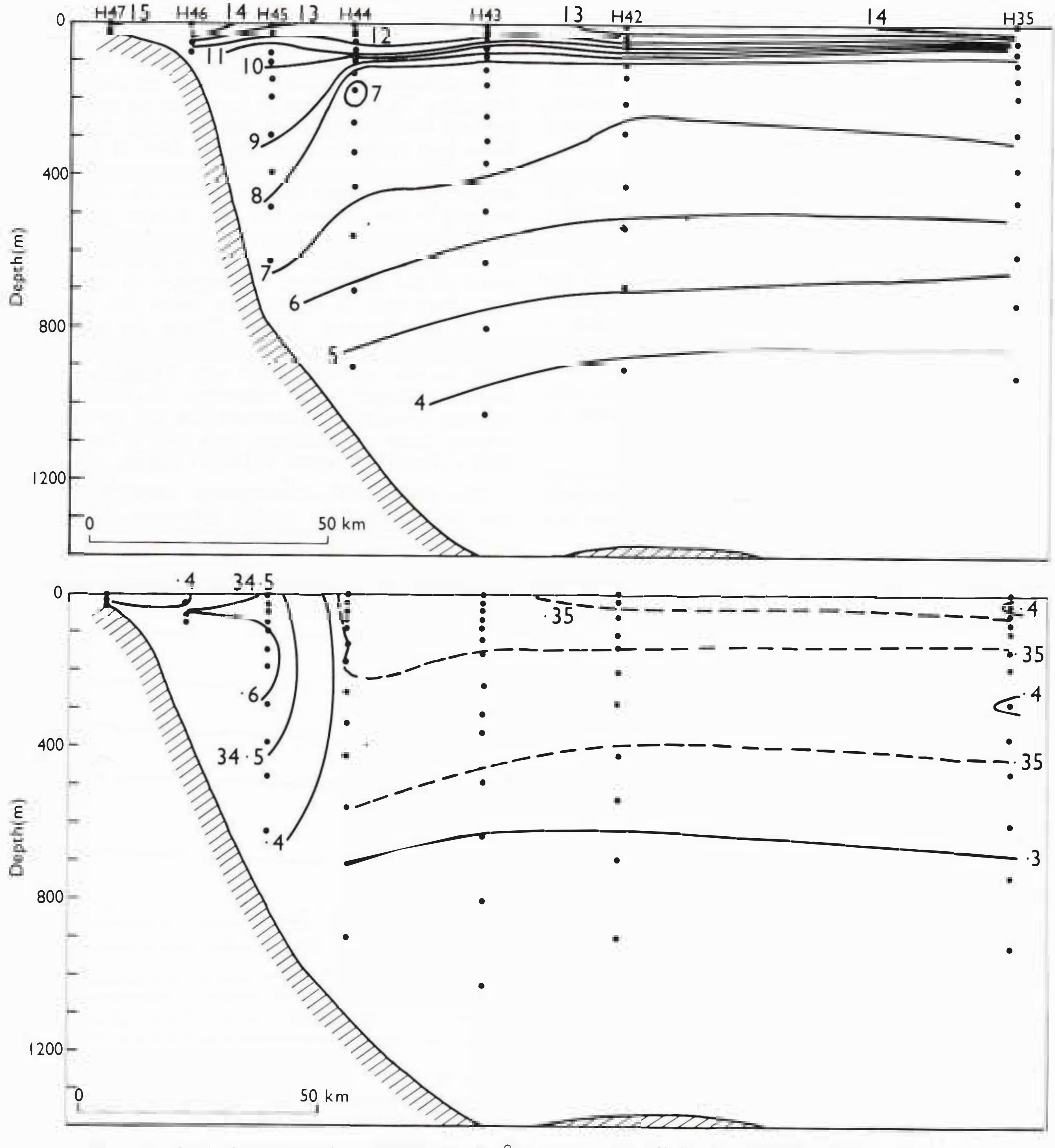

Fig. 11. Vertical cross-sections of temperature (°C) (upper) and salinity (‰) (lower) off the east coast of South Island, New Zealand. (Line joining Stns H35 to H47, Fig. 1.)

THE SUBTROPICAL CONVERGENCE

West of New Zealand

The largest horizontal changes in surface temperature (Fig. 18), surface salinity (Fig. 19), and near-surface maximum salinity (Fig. 20) which occurred perpendicular to the east coast of South Island, marked the position of the Southland Front, and across the Chatham Rise marked the position of the Subtropical Convergence. Off the west coast the position of the Subtropical Convergence was not defined but the water there was of mainly subtropical origin.

There has been some conjecture as to the position of the Subtropical Convergence to the west of New Zealand. Deacon (1937) and Wyrtki (1960, 1962a) placed the Convergence in a line extending north-eastwards from immediately south of Tasmania, towards the west coast of North Island, to the north of Cape Egmont. However, Garner (1959, 1967b) and Fleming (1944) placed the Convergence in a line extending eastwards from immediately south of Tasmania towards the region of Foveaux Strait.

Different opinions as to the position of the Subtropical Convergence may arise, as mentioned by Garner (1967b), from differences in the definition of the Convergence. The region of relatively large meridional gradients of temperature, salinity, and density at the boundary between the Subtropical and Subantarctic Waters (used by Garner 1959, 1967b) would appear to have smaller non-seasonal fluctuations in position and therefore have more significance on the global scale (*see* Deacon 1966) than the boundary between converging non-geostrophic surface currents (used by Wyrtki 1960).

Defining the Subtropical Convergence as the boundary between water masses it follows that a proper analysis of the position of the Convergence in the Tasman Sea will depend on an analysis of the dynamics of the circulation in the Tasman Sea, especially as the main input into this sea appears to be via the southwards-directed East Australian Current off the east coast of Australia. This flow can be envisaged as follows : low density Subtropical Water meets denser Subantarctic Water near Tasmania. Because the flow of Subtropical Water off the east coast of Australia has a larger meridional component than anywhere else at the same latitude in the Tasman Sea, the density gradient between the two water masses near Tasmania (and hence the horizontal velocity shear) will be greater than elsewhere at the Subtropical Convergence in the Tasman Sea. That this is realistic is borne out by Reid's (1961) and Wyrtki's (1962b) figures for geostrophic flow, and Reid's (1965) figures for salinity on constant density surfaces. From near Tasmania the flow obtains a larger zonal component, horizontal mixing will take place in the eastwards flow and the horizontal velocity there will decrease; this also is borne out by Reid's (1961) and Wyrtki's (1962b) figures.

The Subtropical Convergence therefore becomes less well defined as mixing increases, i.e., further

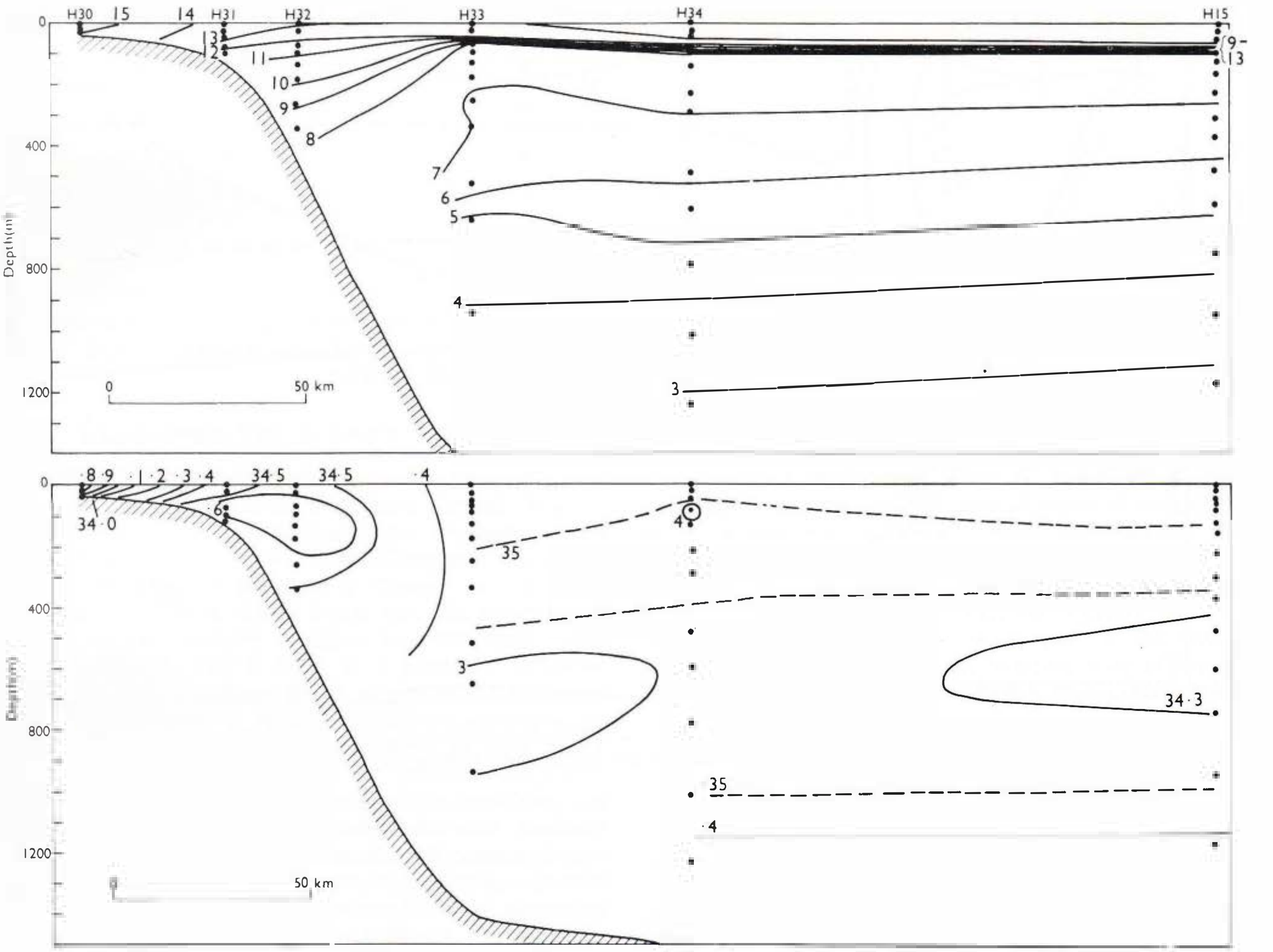

Fig. 12. Vertical cross-sections of temperature (°C) (upper) and salinity (‰) (lower) off the east coast of South Island, New Zealand. (Line joining Stns H15 to H30, Fig. 1.)

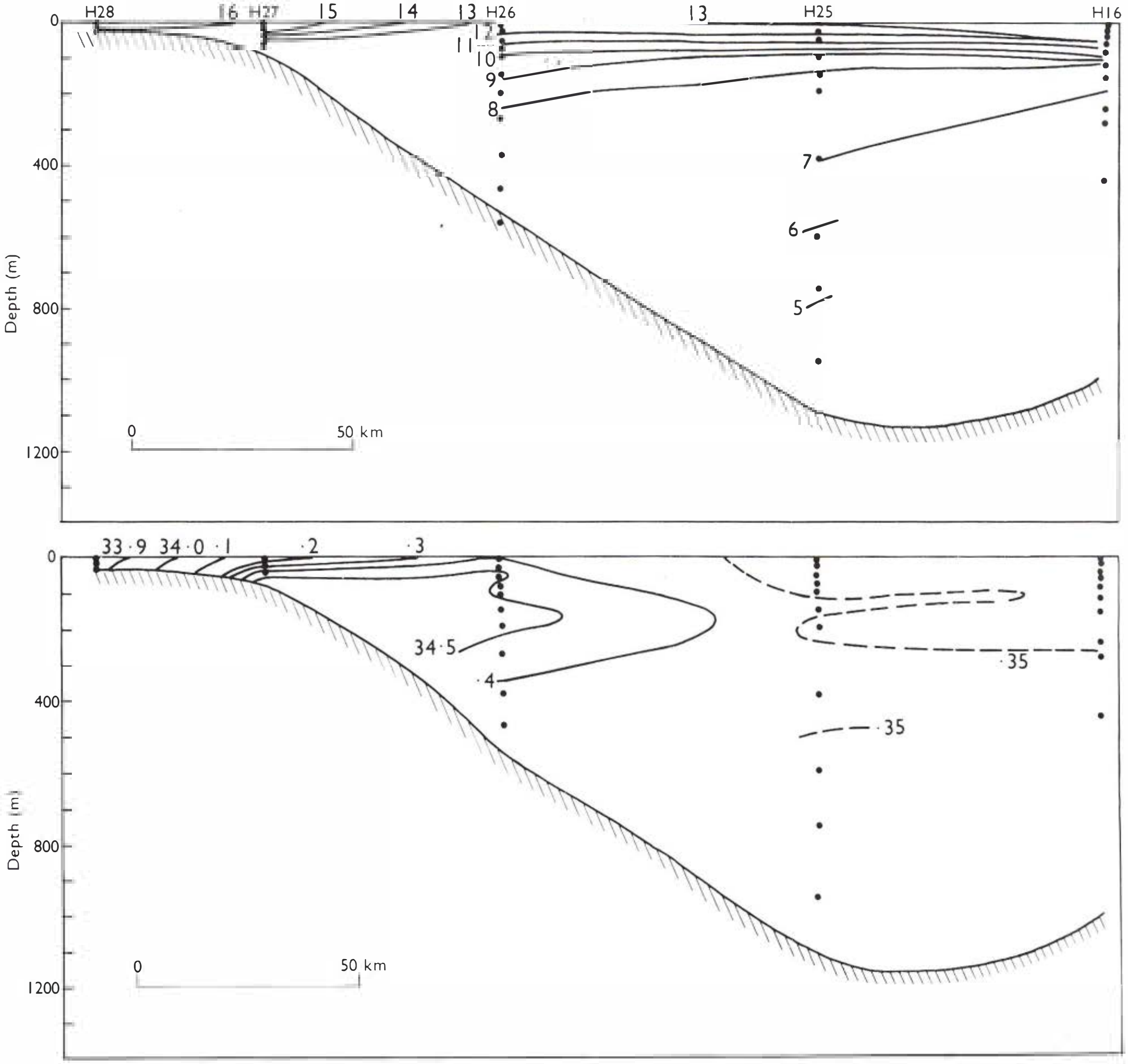

Fig. 13. Vertical cross-sections of temperature (°C) (upper) and salinity (‰) (lower) off the east coast of South Island, New Zealand. (Line joining Stns H16 to H28, Fig. 1.)

from a western boundary for eastward flow. (This is one reason why the Subtropical Convergence is better defined to the east of New Zealand; the other reason is that the Chatham Rise determines the position of the Convergence to the east of New Zealand by limiting the meridional flow of the two water masses.) If we choose a particular dynamic height anomaly contour in the Subtropical Water of the western Tasman Sea then, because of the mixing which will take place mainly across the region of large horizontal density contrast with the lower density Subantarctic Water to the south, the density of the Subtropical Water will be increased as it travels eastwards. Therefore most of this Subtropical Water will be found south of the same dynamic height anomaly contour after it has travelled across the Tasman Sea. By the same reasoning, Subantarctic Water near a particular dynamic height anomaly contour in the western Tasman Sea will be located north of that contour in the eastern Tasman Sea. Therefore a dynamic height anomaly contour near the Subtropical Convergence in (say) mainly Subtropical Water on the western Tasman Sea will be further north of the middle of the Convergence in the eastern Tasman Sea.

All the geopotential topographies of the surface of Tasman Sea relative to 1000 dbar (Reid 1961; Wyrtki 1962b) show the 1.2 dyn m contour forming a tongue-like shape pointing towards the north-east between longitudes 160° and 165°E, with the northernmost point of the tongue at about 44°S. Contours of some hydrological parameters also show tongue-shaped distri-

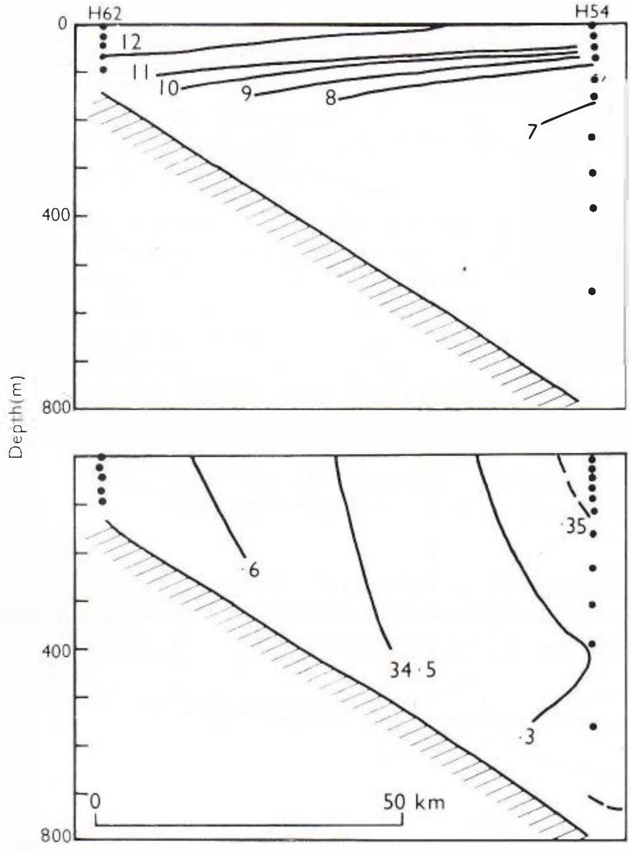

Fig. 14. Vertical cross-sections of temperature (°C) (upper) and salinity (‰) (lower) off the east coast of South Island, New Zealand. (Line joining Stns H54 to H62, Fig. 1.)

butions extending from the south in the south Tasman Sea (Reid 1965) and these tongues could lead to the wrong assumption that the west coast of South Island is bathed by Subantarctic rather than Subtropical Water. The geostrophic flow in this tongue is in a general clockwise direction, water entering the flow from an anticlockwise movement off the south-east coast of Australia and leaving towards the south-west of South Island (*see* Garner 1969, figs 1, 2).

Water in this general movement, having arisen in the East Australian Current, must be of mainly subtropical origin. Essentially Subtropical Water was found off the south-west coast of New Zealand both by Garner (1967b) and by the present survey. In the present survey the water found over the Snares Shelf consisted of warm saline water derived both directly from the Subtropical Water to the north of the Subtropical Convergence and from a sub-surface tongue of water of subtropical origin extending southwards from the Convergence. The Subtropical Convergence must therefore be south of the 1.2 dyn m contour in the eastern Tasman Sea.

Direct confirmation of a southwards flow of Subtropical Water off the south-west coast of New Zealand is given by some recent direct current measurements. On 12 April 1971 near positions latitude 44°S, longitude 168°E on the west coast a parachute drogue at a wire length depth of 500 m showed a mean current velocity of 24 cm s^{-1} at 203°T over a 10 h period. Similar measurements on 13 April 1971 at positions latitude 44°50'S, longitude 167°14'E showed mean current velocities of 40 cm s^{-1} towards 241°T with the drogue at a wire length of 500 m, and 60 cm s^{-1} towards 240°T with the drogue at a wire length of 100 m (Heath 1973). These current measurements made in Subtropical Water are consistent with the general south-westerly geostrophic current down this coast, carrying water of mainly subtropical origin on to and eastwards across the Snares Shelf to contribute to the Southland Current. The Subtropical Convergence lying at the southern edge of this water becomes continuous with the Southland Front off the east coast of South Island, the Southland Front initially arising as the boundary between the oppositely directed movements of Subantarctic Water in the Southland Current and the Bounty-Campbell Gyral (Burling 1961, *see* also Fig. 2).

Deacon (1937) reported that the middle temperature at the Subtropical Convergence boundary was about 57°F (14°C) in summer and 50°F (10°C) in winter, and the middle salinity was 34.9‰, with little seasonal variation. Garner (1959) found that around New Zealand the Convergence followed approximately the isotherms of 15°C in February and 10°C in August, and the isohalines of 34.7‰ to 34.8‰, with little seasonal variation. More recent observations have also indicated that the Convergence is located near to these isoline values (Garner 1967a, b; Heath 1968, 1972b, in press). Garner (1959) also pointed out that the position of largest horizontal temperature and salinity gradients marking the position of the Subtropical Convergence, from Deacon's (1937) and Wyrtki's (1962a) data, is consistent with the Convergence in the Tasman Sea, extending towards Foveaux Strait rather than Cape Egmont, as shown by them.

Wyrtki's (1960) opinion as to the position of the Subtropical Convergence in the Tasman Sea was based on surface-water movements recorded by ships, and later (1962a) on hydrological measurements; in both cases he showed the Convergence extending towards the west coast of North Island. The shallow subsurface maximum salinity layer in the Tasman Sea, which Wyrtki took to lie to the south of the Subtropical Convergence is interpreted by the present author and previous authors (Deacon 1937; Garner 1967b) as lying north of the Convergence as defined here. The region of converging surface currents (Wyrtki 1960) and the region immediately north of where the salinity maximum is found at the surface (Wyrtki 1962a) were found by Wyrtki (1962b) to be in close correspondence, but the position of this region would be highly variable and not as closely linked to the general dynamics of the circulation as that used here to define the Subtropical Convergence.

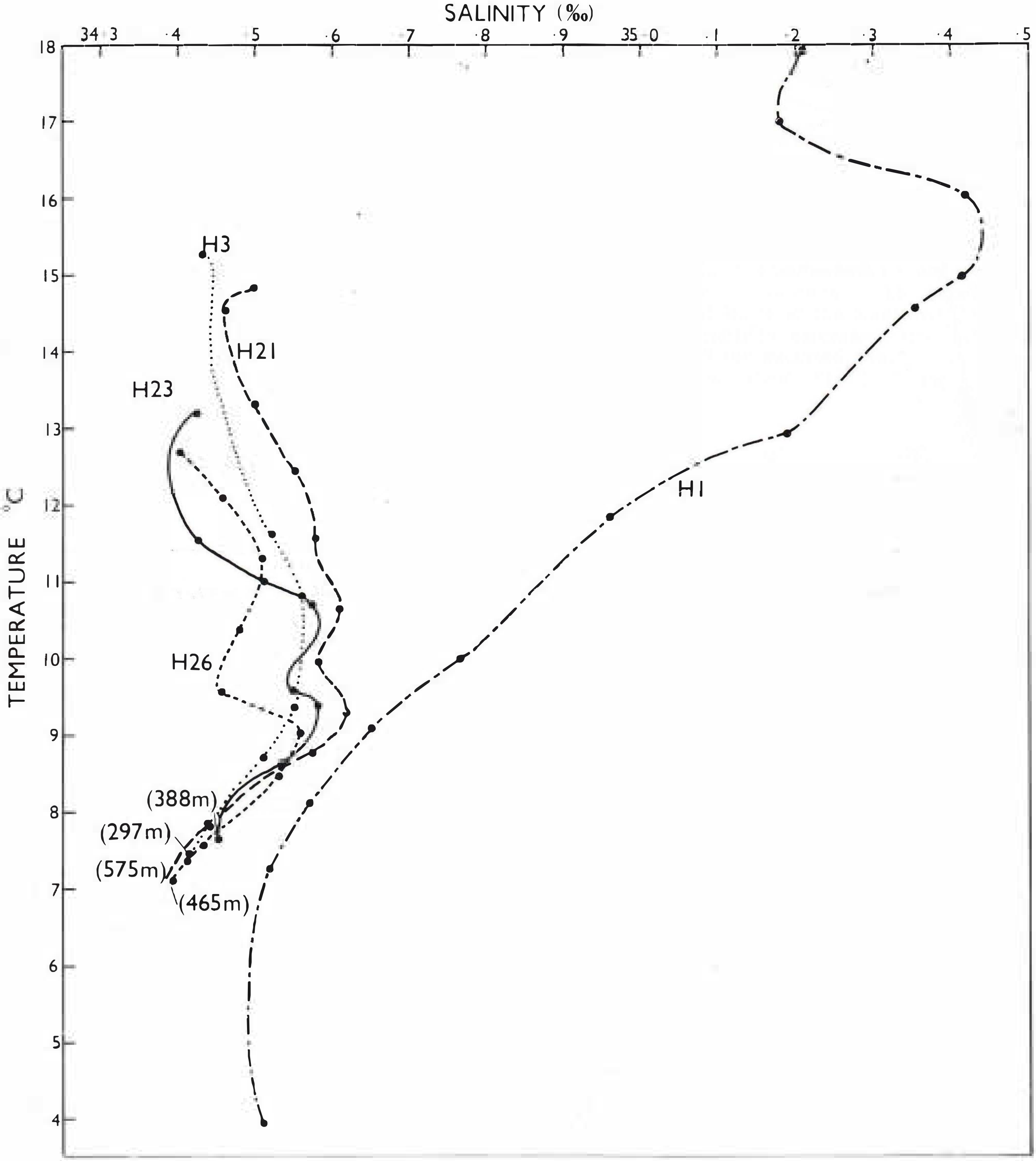

Fig. 15. Temperature (°C) / salinity (‰) curves for Stns H1, H3, H21, H23, H26.

East of New Zealand

Comparison of the surface salinity distribution (Fig. 19) and the near-surface maximum salinity (Fig. 20) shows that the surface water was diluted by coastal runoff along the entire coastline surveyed, the dilution being most pronounced off the west coast, in Foveaux Strait, and in Canterbury Bight. A horizontal tongue of more saline water of mainly subtropical origin extended from the north-west over the Snares Shelf and northwards along the east coast to the Mernoo Gap. This

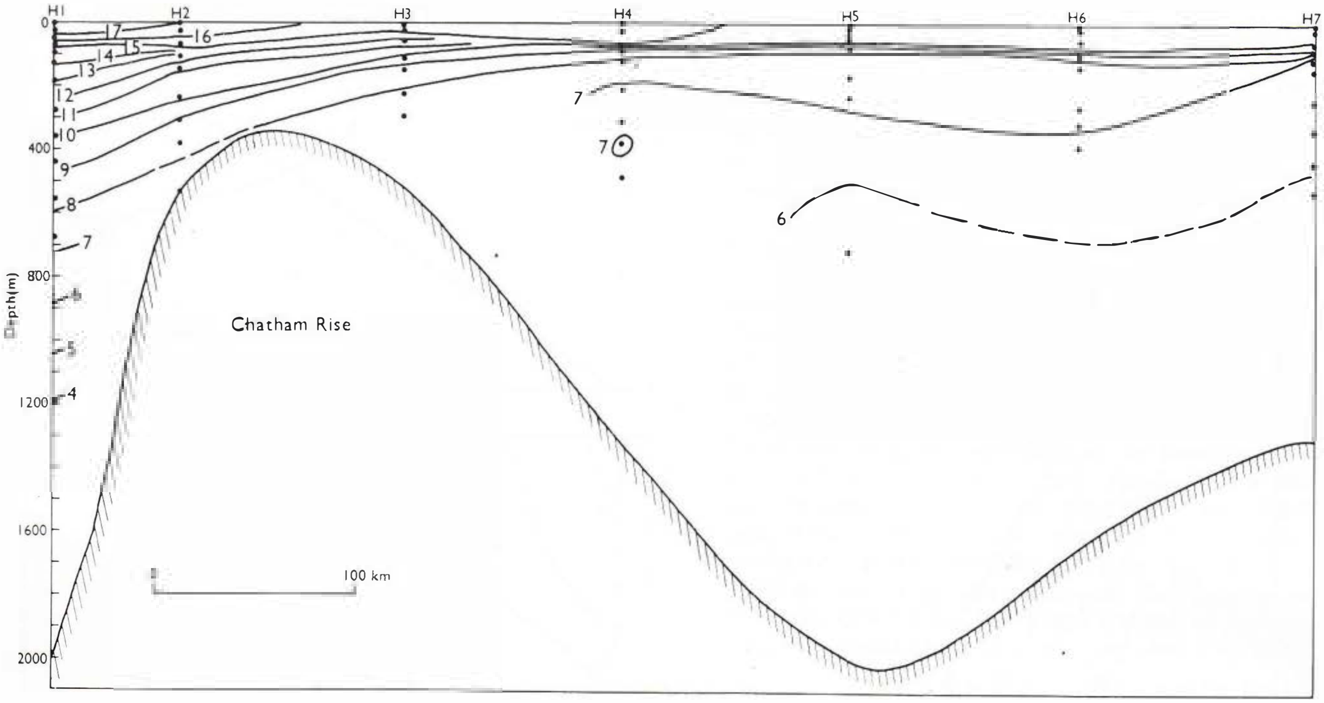

Fig. 16. Sectional temperature (°C) plot across the Chatham Rise. (Line joining Stns H1 to H7, Fig. 1.)

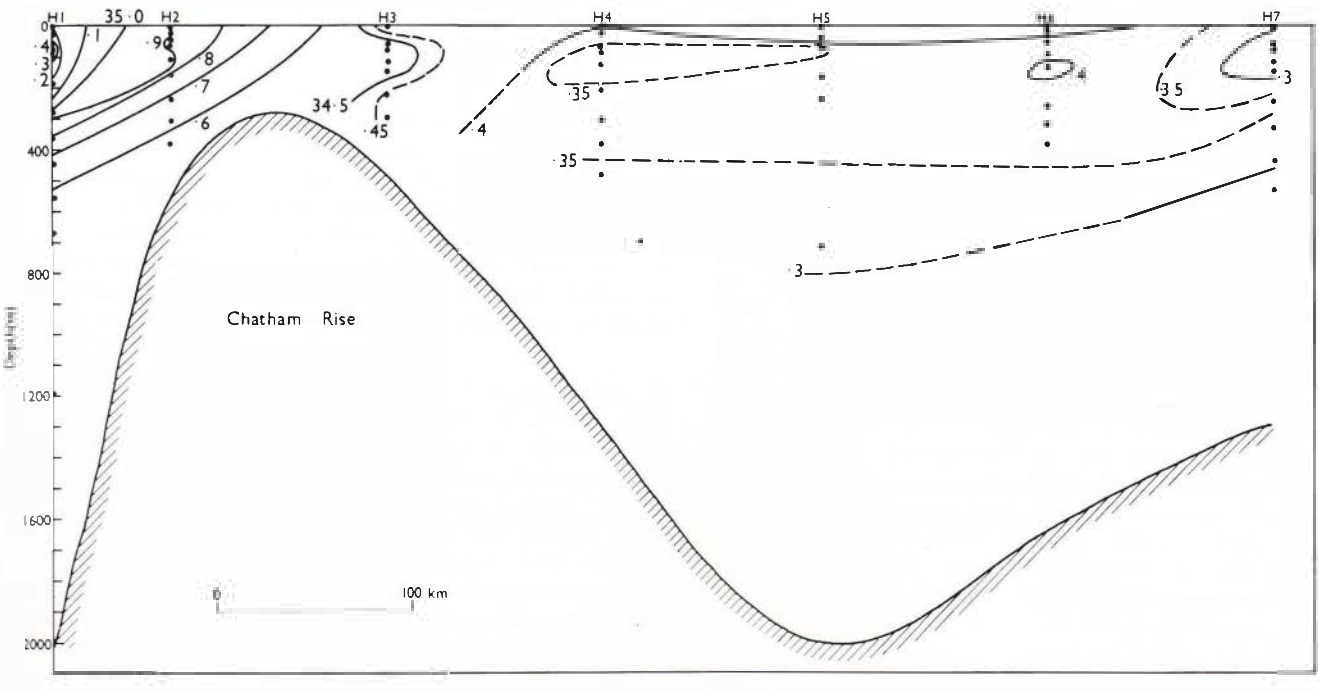

Fig. 17. Sectional salinity (‰) plot across the Chatham Rise. (Line joining Stns H1 to H7. Fig. 1.)

more saline water was bounded inshore by water diluted by coastal runoff and offshore by Subantarctic Surface Water. The outer edge of this tongue lay over the continental slope off the east coast. Offshore from this saline tongue the surface water was relatively isohaline. At many stations in the Subantarctic Water over the Bounty Trough there were slight temperature and salinity inversions between 100 m and 500 m (Appendix). Garner (1967a) and Heath (1968, in press) have shown that in the vertical plane a subsurface tongue of Subtropical Water extends southwards from the Subtropical Convergence in this area, although this tongue does not extend as far south here as that found by Deacon (1937) in the open ocean away from any topographic obstruction such as the Chatham Rise. The diffuse remains of this high salinity warm water probably gave rise to the inversions found by this survey.

Comparison in Fig. 17 of a station in Subtropical Water (H1) with a station in Subantarctic Water (H5) shows that the vertical salinity gradient in the Subantarctic Water is relatively small compared with that in the Subtropical Water.

Surface temperatures in the surveyed region generally decreased with both distance offshore and towards the south (Fig. 18). A distinct region, with temperatures lower than the surrounding water, was found immediately offshore from the continental slope on the east coast. In this region surface salinities were also lower than in the surrounding water. This temperature and salinity contrast would appear to be between the mixed Subantarctic - Subtropical Water of the Southland Current, which had flowed initially northwards then offshore and southwards, and the enclosed Subantarctic Water in the Bounty - Campbell Gyral (Figs 2, 18, 19).

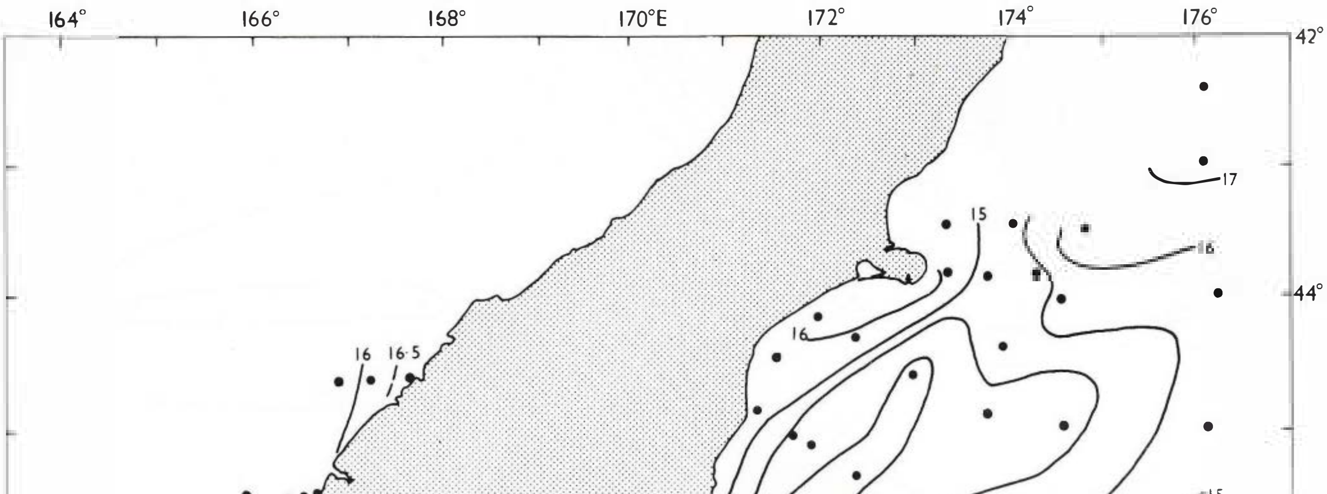

Fig. 18. Isotherms (°C) at the sea surface for data collected in February/March 1970.

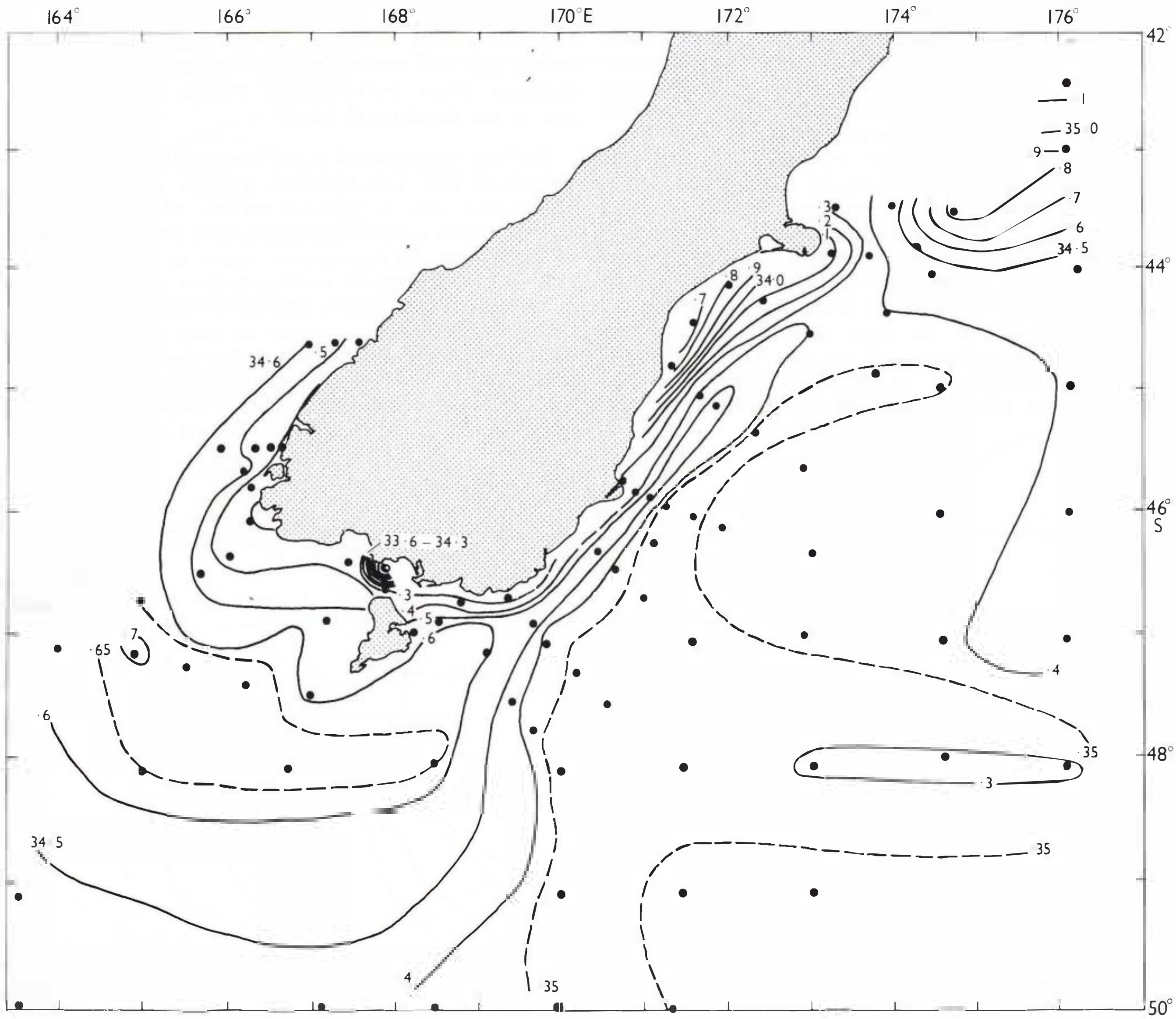

Fig. 19. Isohalines (‰) at the sea surface for data collected in February/March 1970.

CONCLUSIONS

From the present and previous studies an integrated description of the mean circulation around southern New Zealand has been obtained as follows. Subtropical Water in the form of eddies, cast off from the East Australian Current, flows in a general eastwards direction across the Tasman Sea. This warm, saline water meets cooler, less saline Subantarctic Water in the Subtropical Convergence which extends north-eastwards from Tasmania towards about longitude 160°-165°E, then south-eastwards on to the Snares Shelf to the south of New Zealand. Subtropical Water flows northwards along the west coast of New Zealand to the north of about latitude 44°S and southwards to the south of that latitude. Water of mainly subtropical origin flows eastwards through Foveaux Strait and across the Snares Shelf, then north-eastwards on the continental shelf on the east coast of New Zealand, as the Southland Current. Subantarctic Water also flows north-eastwards along the continental slope off the east coast and meets the inshore warmer, more saline water in the Southland Front. The combined north-eastwards flow of coastal, Subtropical, and Subantarctic Waters off the east coast is referred to as the Southland Current. At its southern extremity the Southland Front arises as the boundary between the opposing movements of Subantarctic Water in the Southland Current and the Bounty-Campbell Gyral, but where it is formed as the boundary between mainly Subtropical and Subantarctic Water it can be regarded as being continuous with the Subtropical Convergence of the west coast. Warm, saline water in the Southland Current flows north on the continental shelf, past Banks Peninsula. Some of the cooler, less saline Subantarctic Water flows northwards through the western side of Mernoo Gap and the remainder flows eastwards along the southern flank of the Chatham Rise, meeting the Subtropical Water of the East Cape Current in the Subtropical Convergence. Water in the eastern side of the Mernoo Gap is of mixed Subantarctic and Subtropical origin.

The Southland Current alters its surface hydrological characteristics north of the Mernoo Gap, for, whereas south of this Gap it is defined by a warm, saline surface tongue of water, with coastal water producing the inshore contrast and Subantarctic Water the offshore contrast, north of the Gap it is defined by a cool, low salinity surface tongue. This alteration in characteristics is the result of cool, low salinity Subantarctic Water being brought closer to the surface in flowing northwards through the western side of the Mernoo Gap. The warm, saline water which flows northwards on the continental shelf produces the inshore contrast, and the warm, saline Subtropical Water of the East Cape Current produces the offshore contrast to the north of the Gap.

Flow over the Bounty Trough is weaker than in the Southland Current, and west of longitude 180°E is directed towards the east. Immersed in this flow is the anticlockwise-flowing Bounty-Campbell Gyral centred near latitude 47°S, longitude 171°E, which is about 50-100 km across. East of longitude 180°E a strong northwards flow along the Subantarctic Slope gives rise to a strong clockwise flow over that part of the Bounty Trough.

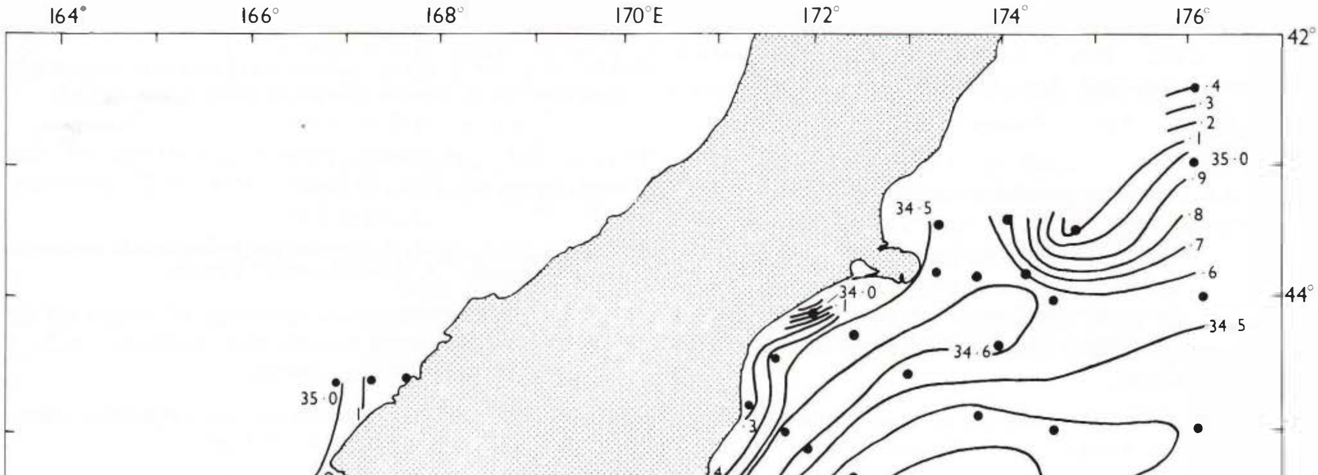

Fig. 20. Contours of the near-surface maximum salinity (‰) for data collected in February/March 1970.

ACKNOWLEDGMENTS

The author is grateful to the cruise personnel from the N.Z. Oceanographic Institute (Messrs A.G. Cole, P.E. Field, B.J. Fowke, W.deL. Main, C. Marott, N.M. Ridgway, N.D. Robertson, and B.S. Shakespeare) and the extremely helpful officers and crew of M.V. *Taranui* (Masters Captain R.D. Matheson and J. Mitchell); the Applied Mathematics Division of the N.Z. Department of Scientific and Industrial Research, for computer facilities; and Miss P. Lawrence of the N.Z. Oceanographic Institute, for preparing the figures.

REFERENCES

BRODIE, J.W. 1960: Coastal surface currents around New Zealand. *N.Z. Jl Geol. Geophys. 3(2)* : 235-52.

BURLING, R.W. 1961: Hydrology of circumpolar waters south of New Zealand. *Mem. N.Z. oceanogr. Inst. 10. (Bull. N.Z. Dep. scient. ind. Res. 143).*

DEACON, G.E.R. 1937: Hydrology of the Southern Ocean. *'Discovery' Rep. 15* : 1-124.

DEACON, G.E.R. 1966: Subtropical Convergence. Pp. 884-85 *in* Fairbridge, R.W. (Editor) 'Encyclopedia of Oceanography'. Reinhold Publishing Corporation, New York. 1021 pp.

FLEMING, C.A. 1944: Molluscan evidence of Pliocene climatic change in New Zealand. *Trans. Proc. R. Soc. N.Z. 74(3)* : 207-20.

GARNER, D.M. 1959: The Subtropical Convergence in New Zealand surface waters. *N.Z. Jl Geol. Geophys. 2(2)* : 315-37.

GARNER, D.M. 1961: Hydrology of New Zealand coastal waters, 1955. *Mem. N.Z. oceanogr. Inst. 8. (Bull. N.Z. Dep. scient. ind. Res. 138).*

GARNER, D.M. 1967a: Hydrology of the southern Hikurangi Trench region. *Mem. N.Z. oceanogr. Inst. 39. (Bull. N.Z. Dep. scient. ind. Res. 177).*

GARNER, D.M. 1967b: Hydrology of the south-east Tasman Sea. *Mem. N.Z. oceanogr. Inst. 48. (Bull. N.Z. Dep. scient. ind. Res. 181).*

GARNER, D.M. 1969: The geopotential topography of the ocean surface around New Zealand. *N.Z. Jl mar. Freshwat. Res. 3(2)* : 209-12.

HEATH, R.A. 1968: Geostrophic currents derived from oceanic density measurements north and south of the Subtropical Convergence east of New Zealand. *N.Z. Jl mar. Freshwat. Res. 2(4)* : 659-77.

HEATH, R.A. 1972a: Choice of reference surface for geostrophic currents around New Zealand. *N.Z. Jl mar. Freshwat. Res. 6(1 & 2)* : 148-77.

HEATH, R.A. 1972b: The Southland Current. *N.Z. Jl mar. Freshwat. Res. 6(4)* : 497-533.

HEATH, R.A. 1973: Direct current measurements around New Zealand. *N.Z. Jl mar. Freshwat. Res. 7(4)* : 331-67.

HEATH, R.A. (in press): Oceanic circulation off the east coast of New Zealand. *Mem. N.Z. oceanogr. Inst. 55.*

HOUTMAN, Th.J. 1966: A note on the hydrological regime in Foveaux Strait. *N.Z. Jl Sci. 9(2)* : 472-83.

JILLETT, J.B. 1969: Seasonal hydrology of waters off the Otago Peninsula, south-eastern New Zealand. *N.Z. Jl mar. Freshwat. Res. 3(3)* : 349-75.

LA FOND, E.C. 1951: Processing oceanographic data. *Publs U.S. hydrogr. Off. 614.* 114 pp.

REID, J.L. 1961: On the geostrophic flow at the surface of the Pacific Ocean with respect to the 1,000 decibar surface. *Tellus 13(4)* : 490-502.

REID, J.L. 1965: Intermediate waters of the Pacific Ocean. *Johns Hopkins oceanogr. Ser. 2* : 85 pp.

RIDGWAY, N.M. 1970: Hydrology of the southern Kermadec Trench region. *Mem. N.Z. oceanogr. Inst. 56. (Bull. N.Z. Dep. scient. ind. Res. 205).*

RIDGWAY, N.M. (in press): Hydrology of the Bounty Island Region. *Mem. N.Z. oceanogr. Inst. 75.*

WYRTKI, K. 1960: The surface circulation in the Coral and Tasman Seas. *Tech. Pap. Div. Fish Oceanogr. C.S.I.R.O. Aust. No. 8.*

WYRTKI, K. 1962a: The subsurface water masses in the western South Pacific Ocean. *Aust. J. mar. Freshwat. Res. 13(1)* : 18-47.

WYRTKI, K. 1962b: Geopotential topographies and associated circulation in the western South Pacific Ocean. *Aust. J. mar. Freshwat. Res. 13(1)* : 89-105.

APPENDIX

NUMERICAL STATION DATA

P is the thermometrically measured pressure in decibars at each sampling point. This is numerically nearly equal to the geometric depths in metres. A more accurate conversion using representative mean density figures (La Fond 1951, p. 8) is as follows:-

pressure (decibars):	200	400	600	800	1000	1500	2000	2500
depth (metres):	199	398	595	793	991	1484	1976	2467

T is the sample temperature in °C x 100

S is the sample salinity in ‰ x 100.

σ_t is the water density reduced to surface pressure isothermally x 100.

σ_{stp} is the *in situ* water density.
The 'σ' value is derived from the relative density, ρ from the relationship $\sigma = (\rho - 1) \times 10^5$ where ρ is the water density in g cm^{-3}.

$\Sigma\Delta D$ is the cumulative anomaly of the geopotential distance between the sea surface and the sample depth in dynamic centimetres.

C is the *in situ* sound velocity in $m\,s^{-1}$ x 100.

Cm is the integral mean sound velocity between the sea surface and the sample depth in $m\,s^{-1}$ x 10.

K is the correction, in metres x 10, to be applied to an echo sounding of a depth corresponding to the depth D on a machine calibrated for a velocity of 1 500 $m\,s^{-1}$

$\Sigma\Delta X = \int_{\rho}^{0} \delta p dp$ is the potential energy anomaly from the sea surface to the sample depth in kg $m\,s^{-4}$ x 10^3 (p is the pressure and δ the specific volume anomaly giving the difference between the actual specific volume and that in a standard ocean at temperature 0°C and salinity at 35‰).

D	T	S	σ_t	σ_{stp}	ΣΔD	C	C_m	K	ΣΔX
H1									
0	1700	3518	2567	2567	0.0	15138	15138	0	0.0
23	1795	3521	2546	2557	5.5	15169	15153	2	64.3
47	1606	3542	2607	2628	10.9	15120	15149	5	252.9
70	1500	3542	2631	2663	15.2	15090	15134	6	501.7
94	1460	3535	2635	2677	19.3	15081	15122	8	841.4
188	1291	3519	2658	2742	34.5	15038	15091	11	2983.8
274	1133	3496	2670	2793	47.1	14996	15068	12	5899.9
360	1000	3477	2679	2842	59.0	14960	15046	11	9666.7
440	912	3465	2684	2883	69.7	14939	15025	8	13916.2
556	812	3457	2694	2946	84.4	14919	15008	3	21270.7
673	728	3452	2702	3008	98.5	14905	14991	-4	29931.2
1200	398	3451	2742	3291	151.1	14857	14943	-46	79165.4
H2									
0	1704	3489	2544	2544	0.0	15135	15135	0	0.0
22	1691	3491	2549	2558	5.5	15135	15135	2	61.2
43	1650	3489	2557	2576	10.7	15125	15133	4	230.2
63	1560	3489	2577	2606	15.9	15103	15126	5	509.1
108	1206	3495	2656	2704	24.0	14994	15095	7	1209.5
152	1049	3477	2671	2739	30.3	14944	15058	6	2037.2
235	1019	3466	2667	2774	42.0	14945	15018	3	4294.2
305	859	3462	2691	2829	51.3	14896	14995	-1	6797.3
380	831	3456	2690	2863	60.5	14898	14975	-6	9949.4

D	T	S	σ_t	σ_{stp}	ΣΔD	C	C_m	K	ΣΔX
H3									
0	1525	3444	2550	2550	0.0	15075	15075	0	0.0
19	1526	3443	2549	2558	4.7	15078	15077	1	45.0
56	1161	3452	2631	2656	12.5	14965	15040	1	339.0
74	1082	3456	2648	2682	15.5	14940	15019	1	532.6
111	937	3455	2673	2723	20.9	14892	14984	-1	1032.8
148	869	3451	2680	2748	25.8	14873	14959	-4	1663.6
222	781	3444	2688	2790	35.0	14851	14927	-11	3376.2
297	735	3442	2693	2829	44.1	14844	14907	-18	5713.9
H4									
0	1571	3440	2537	2537	0.0	15089	15089	0	0.0
21	1550	3439	2541	2550	5.4	15085	15087	1	57.2
64	1560	3434	2535	2563	16.7	15096	15089	4	535.7
85	810	3433	2675	2714	20.8	14839	15059	3	846.3
120	728	3432	2687	2742	25.3	14812	14990	-1	1300.5
209	696	3436	2694	2790	35.8	14814	14914	-12	3037.9
305	697	3438	2696	2835	47.0	14831	14885	-23	5899.4
379	700	3439	3696	2869	55.6	14845	14875	-31	8852.1
489	648	3431	2697	2920	68.5	14841	14868	-43	14467.2
H5									
0	1415	3441	2572	2572	0.0	15039	15039	0	0.0
12	1415	3441	2572	2577	2.7	15041	15040	0	16.4
35	1416	3442	2572	2588	8.0	15046	15042	1	140.0
47	1411	3442	2574	2594	10.7	15046	15043	1	252.4
71	808	3434	2676	2709	15.0	14835	15008	0	506.2
169	711	3438	2694	2771	27.0	14814	14901	-11	1952.6
234	714	3438	2693	2800	34.6	14826	14878	-19	3477.4
716	511	3431	2714	3042	87.9	14822	14842	-75	28799.9
H6									
0	1359	3447	2588	2588	0.0	15022	15022	0	0.0
18	1344	3443	2588	2596	3.8	15019	15021	0	34.5
53	1177	3438	2617	2641	10.8	14967	15002	0	283.0
93	819	3438	2678	2720	17.1	14844	14961	-2	744.5
134	780	3441	2686	2747	22.3	14836	14924	-7	1330.3
261	715	3438	2693	2813	37.5	14831	14880	-21	4342.4
318	706	3438	2694	2840	44.2	14836	14871	-27	6285.1
385	683	3438	2698	2874	52.0	14848	14865	-35	9032.6
H7									
0	1228	3430	2601	2601	0.0	14975	14975	0	0.0
19	1230	3430	2601	2609	3.8	14979	14977	-0	36.2
57	993	3429	2643	2669	10.7	14902	14953	-2	298.6
77	796	3427	2673	2708	13.6	14831	14930	-4	496.9
110	681	3424	2687	2737	17.8	14971	14894	-8	890.4
144	678	3428	2690	2756	21.9	14976	14870	-12	1407.1
249	689	3436	2695	2809	34.2	14818	14844	-26	3819.2
335	672	3433	2695	2848	44.2	14825	14848	-36	6739.7
433	621	3432	2701	2899	55.4	14821	14834	-48	11062.5
531	542	3428	2708	2952	66.2	14804	14830	-60	16255.8
H8									
0	1248	3430	2597	2597	0.0	14982	14982	0	0.0
21	1248	3429	2597	2606	4.3	14985	14984	-0	45.1
64	912	3427	2655	2684	11.9	14873	14947	-2	370.7
85	744	3423	2677	2716	14.9	14812	14921	-4	590.3
115	662	3424	2689	2742	18.6	14785	14889	-9	963.1
H8 continued									
153	668	3429	2692	2763	23.1	14794	14864	-14	1561.4
319	686	3437	2696	2842	42.3	14829	14837	-35	6106.0
519	554	3430	2708	2946	64.6	14808	14830	-59	15435.0
650	484	3432	2718	3016	78.1	14800	14825	-76	23315.7
828	383	3432	2728	3110	94.8	14789	14818	-100	35699.1
H9									
0	1056	3437	2638	2638	0.0	14916	14916	0	0.0
16	1122	3436	2626	2633	2.7	14943	14929	-1	21.9
32	1116	3436	2627	2641	5.5	14942	14936	-1	89.9
48	1003	3436	2647	2668	8.2	14905	14932	-2	197.2
64	833	3436	2674	2703	10.5	14845	14917	-4	327.4
96	741	3435	2687	2731	14.6	14814	14888	-7	651.3
115	719	3439	2693	2746	16.8	14809	14875	-10	887.5
173	716	3438	2693	2772	23.5	14817	14854	-17	1853.8
269	701	3440	2697	2820	34.6	14826	14843	-28	4303.7
347	710	3442	2697	2856	43.6	14843	14841	-37	7070.0
H10									
0	1086	3435	2631	2631	0.0	14926	14926	0	0.0
17	1087	3434	2630	2638	2.9	14930	14928	-1	24.9
33	1091	3434	2630	2645	5.7	14933	14930	-2	94.3
67	1067	3434	2634	2664	11.5	14931	14931	-3	387.5
100	771	3436	2683	2729	16.4	14826	14913	-6	793.9
126	747	3439	2689	2747	19.6	14822	14895	-9	1151.2
178	745	3437	2688	2770	25.8	14828	14874	-15	2100.7
280	712	3443	2697	2826	37.8	14834	14859	-26	4848.2
H11									
0	1089	3437	2632	2632	0.0	14928	14928	0	0.0
23	1091	3435	2631	2641	3.9	14931	14930	-1	45.4
47	1080	3435	2633	2654	8.0	14932	14931	-2	190.3
70	830	3438	2676	2708	11.5	14844	14917	-4	393.7
94	752	3438	2688	2731	14.5	14819	14895	-7	640.2
140	726	3439	2692	2756	20.0	14815	14869	-12	1276.1
185	714	3439	2694	2779	25.2	14818	14856	-18	2124.3
361	700	3440	2697	2862	45.6	14842	14843	-38	7690.1
445	706	3440	2696	2899	55.4	14857	14845	-46	11661.2
H12									
0	1143	3431	2618	2618	0.0	14946	14946	0	0.0
16	1148	3430	2616	2623	2.9	14951	14949	-1	23.7
32	1136	3429	2618	2632	5.9	14948	14949	-1	95.1
48	1128	3429	2619	2641	8.9	14949	14949	-2	213.6
64	913	3428	2655	2685	11.5	14874	14939	-3	363.6
96	773	3432	2680	2724	16.0	14826	14909	-6	719.0
128	701	3431	2690	2748	19.9	14803	14885	-10	1160.1
241	705	3436	2693	2803	33.3	14824	14852	-24	3624.2
286	697	3437	2695	2826	38.5	14827	14847	-29	5012.4
376	666	3434	2697	2869	49.0	14829	14843	-39	8479.6
490	611	3429	2700	2924	62.2	14826	14839	-52	14176.8
641	531	3429	2710	3004	78.9	14817	14835	-70	23631.5
H13									
0	1103	3430	2624	2624	0.0	14932	14932	0	0.0
20	1101	3430	2625	2634	3.5	14934	14933	-1	35.6
39	951	3428	2649	2667	6.7	14883	14921	-2	129.3
59	855	3426	2663	2690	9.7	14850	14903	-4	275.6

H13 continued

D	T	S	σ_t	σ_{stp}	$\Sigma\Delta D$	C	C_m	K	$\Sigma\Delta X$
79	796	3430	2675	2711	12.4	14831	14887	-6	465.1
119	745	3435	2686	2741	17.5	14819	14866	-11	966.9
155	737	3439	2691	2762	21.8	14822	14855	-15	1558.3
190	731	3440	2692	2779	25.9	14825	14850	-19	2269.1
427	643	3434	2700	2895	53.3	14830	14837	-46	10723.9
559	570	3428	2704	2960	68.2	14820	14834	-62	18052.4

H14

D	T	S	σ_t	σ_{stp}	$\Sigma\Delta D$	C	C_m	K	$\Sigma\Delta X$
0	1389	3438	2575	2575	0.0	15030	15030	0	0.0
21	1385	3438	2576	2785	4.7	15032	15031	0	49.6
41	1283	3436	2595	2613	9.0	15001	15024	1	183.7
62	877	3434	2666	2694	12.7	14859	14992	-0	371.7
83	847	3442	2677	2715	15.5	14854	14958	-2	577.8
124	733	3432	2686	2743	20.7	14815	14917	-7	1113.8
243	706	3436	2693	2804	35.0	14824	14869	-21	3735.0
306	707	3438	2694	2834	42.4	14835	14861	-28	5769.7
635	551	3431	2709	3000	79.4	14826	14845	-66	23209.2

H15

D	T	S	σ_t	σ_{stp}	$\Sigma\Delta D$	C	C_m	K	$\Sigma\Delta X$
0	1524	3438	2546	2546	0.0	15074	15074	0	0.0
20	1484	3438	2555	2564	4.9	15064	15049	1	49.7
41	1369	3437	2578	2597	9.8	15030	15058	2	199.7
61	847	3434	2671	2698	13.4	14848	15019	1	382.9
82	803	3432	2676	2713	16.2	14834	14973	-1	583.5
120	727	3435	2689	2744	21.0	14812	14925	-6	1064.2
159	707	3436	2693	2766	25.6	14810	14897	-11	1705.1
221	704	3438	2695	2796	32.8	14821	14874	-19	3071.6
302	697	3438	2696	2834	42.2	14831	14861	-28	5525.6
369	656	3433	2697	2866	49.9	14825	14855	-36	8128.5
477	586	3429	2703	2922	62.2	14814	14847	-49	13305.2
590	520	3429	2711	2982	74.4	14805	14840	-63	19808.9
740	441	3430	2721	3061	89.4	14798	14832	-83	29840.4
947	339	3433	2734	3170	108.3	14790	14824	-111	45706.9
1167	289	3442	2745	3283	125.9	14805	14819	-141	64399.0

H16

D	T	S	σ_t	σ_{stp}	$\Sigma\Delta D$	C	C_m	K	$\Sigma\Delta X$
0	1365	3435	2578	2578	0.0	15022	15022	0	0.0
19	1365	3435	2578	2586	4.2	15025	15024	0	40.2
38	1318	3432	2585	2602	8.4	15013	15021	1	159.4
57	1112	3434	2626	2652	12.1	14945	15007	0	337.8
77	1019	3435	2643	2678	15.5	14915	14987	-1	566.0
116	788	3432	2678	2731	21.2	14835	14949	-4	1115.7
153	709	3431	2688	2759	25.9	14810	14918	-8	1738.2
241	692	3433	2692	2803	36.3	14818	14880	-19	3804.4
277	706	3437	2694	2820	40.6	14829	14873	-23	4903.2
443	708	3439	2695	2898	60.5	14857	14862	-41	12095.4

H17

D	T	S	σ_t	σ_{stp}	$\Sigma\Delta D$	C	C_m	K	$\Sigma\Delta X$
0	1504	3443	2554	2554	0.0	15068	15068	0	0.0
25	1491	3443	2557	2568	6.1	15069	15068	1	76.2
50	1167	3448	2627	2649	11.3	14965	15043	1	273.3
75	1043	3452	2652	2686	15.4	14926	15010	0	532.1
100	1019	3459	2662	2707	19.2	14921	14988	-1	858.8
145	915	3455	2676	2742	25.4	14891	14963	-4	1623.4
194	893	3457	2681	2769	31.8	14891	14944	-7	2706.2
290	813	3449	2687	2819	43.9	14875	14924	-15	5641.4
388	753	3442	2691	2868	56.0	14867	14911	-23	9741.9

H18

D	T	S	σ_t	σ_{stp}	$\Sigma\Delta D$	C	C_m	K	$\Sigma\Delta X$
0	1490	3436	2552	2552	0.0	15063	15063	0	0.0
25	1417	3442	2572	2583	5.9	15045	15054	1	74.3
50	1184	3458	2631	2654	10.9	14972	15031	1	262.7

H19

D	T	S	σ_t	σ_{stp}	$\Sigma\Delta D$	C	C_m	K	$\Sigma\Delta X$
0	1603	3407	2505	2505	0.0	15095	15095	0	0.0
19	1483	3433	2551	2560	5.1	15063	15079	1	48.8
39	1408	3442	2574	2592	9.8	15044	15066	2	186.8
58	1270	3456	2613	2639	13.8	15003	15052	2	379.3

H20

D	T	S	σ_t	σ_{stp}	$\Sigma\Delta D$	C	C_m	K	$\Sigma\Delta X$
0	1523	3434	2543	2543	0.0	15073	15073	0	0.0
25	1492	3436	2552	2563	6.3	15068	15071	1	78.7
50	1282	3453	2608	2631	11.8	15005	15054	2	286.5

H21

D	T	S	σ_t	σ_{stp}	$\Sigma\Delta D$	C	C_m	K	$\Sigma\Delta X$
0	1467	3446	2565	2565	0.0	15057	15057	0	0.0
24	1482	3450	2564	2575	5.6	15065	15061	1	67.8
48	1246	3455	2617	2639	10.7	14993	15045	1	250.4
71	1157	3458	2636	2668	14.8	14966	15024	1	493.7
95	1131	3458	2641	2684	18.8	14961	15008	1	826.1
142	1063	3461	2656	2720	26.2	14945	14990	-1	1708.4
177	999	3458	2665	2745	31.4	14927	14979	-2	2535.3
260	931	3462	2679	2797	42.9	14917	14961	-7	5042.0
342	877	3457	2684	2839	53.6	14909	14949	-12	8266.5
430	851	3454	2686	2880	65.0	14913	14941	-17	12654.5
575	710	3439	2695	2956	83.2	14881	14930	-27	21820.1

H22

D	T	S	σ_t	σ_{stp}	$\Sigma\Delta D$	C	C_m	K	$\Sigma\Delta X$
0	1691	3485	2544	2544	0.0	15131	15131	0	0.0
24	1664	3483	2549	2559	6.0	15126	15128	2	72.8
48	1478	3491	2597	2618	11.5	15074	15114	4	270.2
71	1325	3516	2648	2680	15.7	15030	15094	4	518.9
95	1312	3516	2651	2694	19.4	15031	15078	5	830.8
141	1241	3507	2658	2722	26.5	15012	15059	6	1660.2
187	1171	3497	2664	2748	33.3	14995	15045	6	2774.9
280	995	3467	2672	2799	46.5	14944	15020	4	5868.5

H23

D	T	S	σ_t	σ_{stp}	$\Sigma\Delta D$	C	C_m	K	$\Sigma\Delta X$
0	1456	3446	2567	2567	0.0	15053	15053	0	0.0
24	1324	3442	2591	2602	5.3	15013	15033	1	63.8
48	1154	3442	2624	2646	9.9	14959	15009	0	232.2
72	1102	3451	2641	2674	14.1	14945	14990	-0	479.8
97	1078	3457	2650	2694	18.1	14942	14978	-1	818.7
146	956	3454	2669	2735	25.3	14906	14960	-4	1699.8
195	940	3458	2674	2763	32.1	14908	14947	-7	2847.2
290	862	3453	2683	2815	44.6	14895	14932	-13	5885.6
388	764	3445	2692	2868	56.9	14872	14920	-21	10049.1

H24

D	T	S	σ_t	σ_{stp}	$\Sigma\Delta D$	C	C_m	K	$\Sigma\Delta X$
0	1491	3440	2555	2555	0.0	15064	15064	0	0.0
25	1362	3438	2581	2592	5.8	15026	15045	1	72.6
50	1132	3441	2628	2650	10.7	14951	15017	1	258.8
75	1011	3449	2655	2689	14.8	14914	14989	-1	514.3
100	967	3455	2668	2713	18.4	14902	14968	-2	831.7
148	949	3463	2677	2744	25.0	14904	14947	-5	1639.3
198	873	3456	2684	2774	31.4	14883	14934	-9	2755.1
295	807	3450	2689	2823	43.5	14873	14915	-15	5730.7

H24 continued

D	T	S	σ_t	σ_{stp}	ΣΔD	C	C_m	K	ΣΔX
390	759	3444	2692	2869	55.1	14870	14905	-25	9712.3
487	727	3440	2693	2915	67.0	14873	14898	-33	14909.0

H25

D	T	S	σ_t	σ_{stp}	ΣΔD	C	C_m	K	ΣΔX
0	1339	3433	2581	2581	0.0	15013	15013	0	0.0
24	1281	3431	2592	2602	5.1	14997	15005	0	61.8
48	1129	3431	2621	2642	9.8	14949	14989	-0	231.8
72	996	3432	2645	2677	14.0	14905	14968	-2	479.4
97	854	3434	2669	2714	17.7	14857	14946	-4	794.4
146	783	3439	2684	2751	24.1	14839	14913	-8	1574.6
194	711	3434	2690	2779	29.9	14818	14892	-14	2568.3
380	700	3439	2696	2870	51.9	14845	14862	-35	8874.4
599	597	3431	2703	2977	77.1	14838	14855	-58	21222.4
749	516	3432	2714	3057	93.5	14829	14850	-75	32221.8
949	437	3432	2723	3158	113.7	14831	14846	-97	49380.7

H26

D	T	S	σ_t	σ_{stp}	ΣΔD	C	C_m	K	ΣΔX
0	1274	3440	2600	2600	0.0	14992	14992	0	0.0
25	1212	3446	2617	2628	4.8	14977	14985	-0	60.6
50	1135	3451	2635	2658	9.3	14954	14975	-1	227.5
74	1037	3448	2650	2684	13.2	14923	14963	-2	469.4
98	959	3445	2661	2706	16.8	14898	14950	-3	780.3
145	903	3456	2679	2745	23.2	14886	14931	-7	1566.5
190	850	3453	2685	2771	29.0	14872	14919	-10	2525.5
265	759	3443	2691	2812	38.2	14849	14902	-17	4616.6
370	712	3439	2694	2863	50.7	14848	14887	-28	8601.1
465	707	3439	2695	2907	62.0	14860	14880	-37	13330.3

H27

D	T	S	σ_t	σ_{stp}	ΣΔD	C	C_m	K	ΣΔX
0	1588	3414	2513	2513	0.0	15091	15091	0	0.0
20	1501	3428	2543	2552	5.4	15069	15080	1	53.9
39	1378	3443	2581	2599	9.9	15034	15066	2	187.5
49	1268	3455	2613	2635	11.9	15000	15056	2	278.0

H28

D	T	S	σ_t	σ_{stp}	ΣΔD	C	C_m	K	ΣΔX
0	1632	3384	2480	2480	0.0	15101	15101	0	0.0
5	1607	3385	2487	2489	1.5	15095	15098	0	3.9
10	1605	3387	2489	2493	3.1	15094	15096	1	15.4
15	1600	3389	2491	2498	4.6	15095	15096	1	34.6

H29

D	T	S	σ_t	σ_{stp}	ΣΔD	C	C_m	K	ΣΔX
0	1518	3364	2491	2491	0.0	15063	15063	0	0.0
10	1516	3365	2492	2496	3.0	15064	15063	0	15.2
19	1531	3404	2518	2527	5.6	15075	15066	1	53.4
29	1360	3441	2583	2596	8.1	15026	15061	1	113.1
39	1345	3448	2592	2609	10.3	15024	15052	1	186.0

H30

D	T	S	σ_t	σ_{stp}	ΣΔD	C	C_m	K	ΣΔX
0	1553	3378	2494	2494	0.0	15076	15076	0	0.0
9	1553	3378	2494	2498	2.7	15077	15076	0	12.2
19	1556	3377	2492	2501	5.7	15080	15077	1	54.8
28	1553	3377	2493	2505	8.5	15080	15078	1	119.2
37	1464	3423	2548	2564	11.0	15059	15076	2	200.6

H31

D	T	S	σ_t	σ_{stp}	ΣΔD	C	C_m	K	ΣΔX
0	1380	3446	2583	2583	0.0	15028	15028	0	0.0
23	1378	3445	2583	2593	5.0	15031	15030	0	57.7
46	1362	3463	2600	2620	9.8	15033	15031	1	224.9

H31 continued

D	T	S	σ_t	σ_{stp}	ΣΔD	C	C_m	K	ΣΔX
70	1245	3463	2623	2655	14.4	14997	15025	1	492.3
93	1193	3460	2631	2673	18.5	14983	15016	1	825.6

H32

D	T	S	σ_t	σ_{stp}	ΣΔD	C	C_m	K	ΣΔX
0	1335	3453	2598	2598	0.0	15014	15014	0	0.0
23	1264	3457	2615	2625	4.5	14994	15004	0	51.7
45	1274	3463	2618	2638	8.6	15003	15002	0	191.6
69	1146	3465	2644	2675	12.7	14963	14995	-0	429.4
91	1123	3463	2646	2688	16.3	14957	14987	-1	712.2
130	1067	3463	2657	2715	22.3	14944	14976	-2	1381.3
175	1029	3465	2665	2744	29.0	14939	14967	-4	2393.4
260	908	3457	2679	2797	40.7	14907	14953	-8	4947.1
340	807	3449	2688	2843	51.0	14881	14939	-14	8025.9

H33

D	T	S	σ_t	σ_{stp}	ΣΔD	C	C_m	K	ΣΔX
0	1282	3435	2594	2594	0.0	14994	14994	0	0.0
21	1271	3434	2596	2605	4.3	14994	14994	-0	45.5
43	1249	3434	2600	2619	8.8	14990	14993	-0	189.3
64	789	3432	2678	2707	12.3	14827	14965	-1	375.6
86	748	3433	2684	2724	15.0	14815	14928	-4	583.4
129	712	3433	2690	2749	20.2	14807	14889	-10	1142.1
170	705	3434	2691	2769	25.1	15811	14869	-15	1867.3
250	696	3436	2694	2809	34.5	14822	14852	-25	3835.8
331	700	3438	2695	2847	43.9	14837	14847	-34	6583.9
515	671	3434	2696	2931	65.7	14855	14846	-53	15786.8
640	483	3427	2714	3008	79.5	14797	14842	-67	23792.0
938	392	3430	2726	3157	108.7	14810	14830	-106	46823.2

H34

D	T	S	σ_t	σ_{stp}	ΣΔD	C	C_m	K	ΣΔX
0	1407	3437	2570	2570	0.0	15036	15036	0	0.0
22	1377	3436	2576	2586	5.0	15029	15033	0	55.0
44	1319	3435	2587	2607	9.8	15015	15027	1	214.7
88	814	3443	2683	2723	17.3	14841	14978	-1	708.3
132	765	3437	2685	2746	22.7	14830	14930	-6	1308.5
220	711	3436	2692	2793	33.3	14821	14888	-16	3176.4
284	703	3438	2695	2825	40.8	14830	14874	-24	5068.5
478	629	3432	2700	2919	63.3	14832	14856	-46	13611.1
600	561	3431	2708	2983	76.9	14823	14851	-60	20944.0
775	468	3431	2719	3074	95.1	14814	14843	-81	33459.1
1008	346	3435	2735	3198	116.6	14802	14835	-111	52662.6
1238	291	3444	2747	3316	135.1	14817	14831	-140	73390.1

H35

D	T	S	σ_t	σ_{stp}	ΣΔD	C	C_m	K	ΣΔX
0	1450	3439	2563	2563	0.0	15050	15050	0	0.0
24	1444	3440	2565	2576	5.6	15052	15051	1	68.0
48	884	3435	2666	2687	10.1	14861	15003	0	230.4
72	806	3433	2676	2709	13.4	14834	14951	-2	425.6
97	776	3432	2680	2724	16.6	14827	14920	-5	698.8
145	736	3436	2689	2755	22.6	14820	14888	-11	1418.7
190	736	3437	2689	2776	28.0	14827	14872	-16	2324.3
285	707	3440	2696	2826	39.2	14832	14858	-27	4985.1
377	690	3438	2697	2869	49.9	14841	14853	-37	8520.3
468	624	3432	2701	2915	60.3	14828	14849	-47	12946.0
602	540	3430	2710	2986	75.1	14815	14843	-63	20842.0
740	450	3430	2720	3060	89.2	14802	14836	-81	30294.7
923	362	3434	2732	3157	106.0	14795	14829	-105	44322.7

H36

D	T	S	σ_t	σ_{stp}	ΣΔD	C	C_m	K	ΣΔX
0	1304	3436	2591	2591	0.0	15002	15002	0	0.0
23	1312	3435	2588	2599	4.8	15008	15005	0	56.0

D	T	S	σ_t	σ_{stp}	ΣΔD	C	C_m	K	ΣΔX
H36 continued									
47	1053	3431	2634	2655	9.4	14922	14984	-0	217.0
70	828	3436	2675	2707	12.9	14843	14951	-2	420.1
94	763	3433	2682	2725	16.0	14822	14920	-5	672.9
141	736	3438	2690	2755	21.7	14819	14887	-11	1345.9
185	709	3436	2692	2777	26.9	14816	14870	-16	2191.0
275	703	3439	2696	2821	37.4	14828	14855	-27	4600.8
359	700	3439	2696	2860	47.1	14842	14850	-36	7696.3
444	671	3435	2697	2900	57.1	14842	14848	-45	11692.4
572	593	3429	2702	2964	71.9	14831	14846	-59	19204.3
613	508	3430	2713	2995	76.3	14805	14844	-64	21832.9
889	415	3431	2724	3133	103.6	14812	14833	-99	42309.2
H37									
0	1316	3434	2587	2587	0.0	15006	15006	0	0.0
19	1312	3434	2588	2596	4.0	15008	15007	0	38.6
38	1305	3434	2589	2606	8.1	15008	15007	0	154.1
57	1216	3432	2605	2631	12.0	14981	15003	0	339.7
77	1001	3432	2644	2679	15.6	14908	14988	-1	580.8
116	809	3433	2676	2728	21.3	14843	14950	-4	1133.5
154	710	3432	2689	2760	26.1	14811	14919	-8	1779.4
231	694	3437	2695	2801	35.1	14818	14884	-18	3520.2
342	610	3429	2700	2857	47.7	14801	14860	-32	7132.1
599	498	3429	2714	2989	75.2	14797	14834	-66	20072.1
782	403	3431	2726	3086	93.0	14789	14824	-92	32323.8
H38									
0	1215	3434	2607	2607	0.0	14972	14972	0	0.0
16	1225	3434	2605	2612	3.1	14978	14975	-0	25.1
32	1202	3434	2609	2624	6.2	14972	14975	-1	100.2
48	1152	3433	2618	2639	9.3	14957	14971	-1	221.6
64	1065	3433	2634	2663	12.1	14930	14965	-2	381.5
96	738	3434	2687	2731	16.8	14813	14933	-4	755.5
192	703	3437	2694	2782	28.1	14815	14873	-16	2391.5
256	701	3439	2696	2813	35.5	14824	14860	-24	4045.7
311	713	3440	2695	2837	41.9	14839	14855	-30	5854.9
421	694	3439	2697	2889	54.8	14849	14852	-42	10567.5
553	621	3433	2702	2955	70.0	14840	14840	-55	17998.4
728	533	3431	2711	3044	89.4	14833	14847	-74	30388.1
H39									
0	1203	3436	2611	2611	0.0	14968	14968	0	0.0
18	1206	3436	2610	2618	3.4	14972	14970	-0	31.1
36	1206	3436	2610	2626	6.9	14975	14972	-1	124.7
54	1202	3436	2611	2635	10.3	14977	14973	-1	281.0
72	1114	3434	2626	2658	13.7	14947	14970	-1	491.7
108	877	3436	2667	2717	19.4	14868	14949	-4	1008.2
216	700	3436	2694	2793	33.3	14817	14896	-15	3249.9
288	700	3438	2695	2827	41.6	14829	14877	-24	5361.2
361	699	3438	2695	2860	50.2	14841	14869	-32	8129.5
491	709	3440	2695	2919	65.6	14866	14865	-44	14699.7
H40									
0	1367	3456	2593	2593	0.0	15025	15025	0	0.0
23	1371	3455	2592	2602	4.8	15030	15028	0	55.2
47	1138	3490	2665	2686	9.0	14960	15011	0	202.7
70	1070	3465	2658	2689	12.3	14936	14990	-0	397.7
94	1060	3465	2659	2702	15.9	14937	14976	-1	688.8
113	1043	3466	2663	2714	18.6	14934	14969	-2	975.6

D	T	S	σ_t	σ_{stp}	ΣΔD	C	C_m	K	ΣΔX
H41									
0	1244	3437	2603	2603	0.0	14982	14982	0	0.0
18	1237	3437	2605	2613	3.5	14983	14982	-0	32.0
37	1236	3436	2604	2621	7.3	14985	14983	-0	135.5
55	1165	3435	2617	2642	10.7	14964	14980	-1	295.0
73	903	3434	2662	2695	13.7	14871	14965	-2	485.8
110	736	3435	2688	2738	18.6	14814	14923	-6	934.0
219	704	3438	3695	2795	31.5	14819	14870	-19	3048.0
284	706	3440	2696	2826	39.0	14831	14860	-27	4936.8
351	701	3440	2697	2857	46.7	14840	14855	-34	7399.8
449	689	3438	2697	2902	58.2	14851	14853	-44	11981.5
566	624	3433	2701	2960	71.8	14844	14852	-56	18881.3
746	541	3432	2711	3052	91.8	14840	14850	-75	32005.6
H42									
0	1350	3437	2582	2582	0.0	15017	15017	0	0.0
17	1358	3438	2581	2589	3.7	15023	15020	0	31.6
35	1239	3433	2601	2617	7.5	14986	15012	0	130.1
52	1140	3431	2619	2642	10.7	14953	14998	-0	273.0
104	768	3433	2682	2729	18.8	14826	14944	-4	904.4
138	735	3435	2688	2751	23.0	14818	14913	-8	1411.7
207	710	3438	2694	2789	31.2	14820	14882	-16	2820.8
287	689	3439	2697	2829	40.4	14824	14865	-26	5094.8
422	663	3434	2697	2890	56.0	14836	14854	-41	10613.3
535	594	3430	2703	2948	68.9	14827	14849	-54	16805.6
695	504	3430	2714	3033	86.2	14816	14843	-73	27430.5
903	381	3431	2728	3143	106.4	14799	14835	-100	43595.7
H43									
0	1289	3434	2592	2592	0	14997	14997	0	0.0
20	1273	3434	2595	2604	4.1	14994	14996	-0	41.5
40	1124	3432	2622	2640	8.0	14946	14983	-0	157.8
60	975	3432	2648	2676	11.4	14896	14962	-2	327.1
80	810	3433	2675	2712	14.3	14637	14938	-3	529.1
120	732	3433	2687	2742	19.3	14813	14900	-8	1034.9
160	711	3436	2692	2765	24.1	14812	14878	-13	1702.2
240	709	3438	2694	2804	33.4	14826	14858	-23	3470.9
307	702	3438	2695	2835	41.2	14833	14852	-30	5710.4
363	717	3438	2693	2859	47.9	14848	14850	-36	7932.4
492	647	3434	2699	2924	63.1	14841	14849	-50	14432.2
626	567	3430	2706	2993	78.2	14831	14846	-64	22902.9
804	466	3432	2720	3089	96.9	14818	14841	-85	36232.0
1025	360	3433	2732	3203	117.6	14811	14835	-112	55203.8
H44									
0	1236	3433	2602	2602	0.0	14979	14979	0	0.0
22	1241	3433	2601	2611	4.4	14983	14981	-0	48.5
43	1221	3433	2605	2624	8.6	14980	14981	-1	184.8
65	1108	3433	2626	2655	12.7	14945	14975	-1	408.5
87	975	3434	2650	2689	16.4	14901	14962	-2	688.3
130	744	3435	2687	2746	22.4	14820	14928	-6	1336.3
174	697	3434	2692	2772	27.6	14809	14899	-12	2133.9
261	703	3438	2695	2814	37.7	14827	14872	-22	4338.4
340	703	3438	2695	2850	47.0	14839	14863	-31	7113.6
425	703	3439	2696	2890	57.0	14852	14860	-40	10951.5
557	671	3435	2697	2951	72.7	14862	14859	-52	18662.2
705	581	3430	2705	3027	90.0	14849	14858	-67	29548.8
903	488	3431	2716	3129	111.5	14844	14856	-87	46885.8

D	T	S	σ_t	σ_{stp}	ΣΔD	C	C_m	K	ΣΔX
H45									
0	1364	3453	2592	2592	0.0	15024	15024	0	0.0
24	1292	3459	2611	2622	4.8	15004	15014	0	57.7
49	1153	3454	2634	2656	9.3	14961	14998	-0	223.0
73	1079	3454	2647	2680	13.2	14938	14982	-1	463.7
97	1023	3464	2665	2709	16.8	14924	14969	-2	769.9
146	959	3463	2675	2741	23.6	14908	14951	-5	1589.6
194	937	3462	2678	2766	29.9	14908	14940	-8	2670.8
292	912	3459	2680	2812	42.9	14914	14930	-14	5810.8
387	852	3453	2685	2860	55.3	14907	14926	-19	10023.9
479	767	3445	2691	2909	66.9	14888	14920	-26	15072.1
625	726	3441	2694	2978	85.1	14895	14913	-36	25083.2
H46									
0	1460	3439	2561	2561	0.0	15054	15054	0	0.0
25	1458	3439	2561	2572	5.9	15038	15056	1	74.6
50	1262	3463	2620	2643	11.2	14999	15042	1	272.9
75	1162	3463	2639	2673	15.6	14970	15023	1	546.4
H47									
0	1500	3435	2549	2549	0.0	15066	15066	0	0.0
10	1474	3436	2555	2560	2.4	15059	15063	0	12.3
20	1440	3443	2568	2577	4.8	15051	15059	1	48.1
H48									
0	1568	3432	2532	2532	0.0	15087	15087	0	0.0
20	1422	3453	2580	2589	4.8	15046	15067	1	48.8
39	1335	3467	2609	2626	8.8	15023	15051	1	165.3
59	1332	3467	2609	2636	12.7	15025	15042	2	356.0
H49									
0	1463	3456	2573	2573	0.0	15057	15057	0	0.0
24	1221	3465	2630	2640	4.8	14981	15019	0	57.7
48	1118	3438	2628	2650	9.0	14946	14991	-0	209.0
72	1069	3466	2659	2691	12.9	14936	14974	-1	442.2
97	1066	3466	2659	2703	16.5	14939	14965	-2	754.2
H50									
0	1328	3439	2588	2588	0.0	15010	15010	0	0.0
24	1123	3436	2626	2636	4.6	14943	14977	-0	56.2
48	1082	3441	2637	2659	8.8	14934	14957	-1	205.5
71	1051	3442	2643	2675	12.6	14926	14949	-2	431.4
95	1020	3445	2651	2694	16.4	14920	14942	-4	747.9
143	905	3455	2678	2743	23.3	14887	14929	-7	1565.3
190	874	3458	2685	2772	29.3	14882	14918	-10	2564.6
185	750	3441	2690	2775	28.7	14883	14920	-10	2450.4
385	727	3441	2694	2869	52.5	14856	14880	-31	9251.9
470	713	3440	2695	2909	62.7	14864	14877	-39	13604.7
563	681	3436	2696	2953	73.9	14866	14875	-47	19374.3
H51									
0	1308	3433	2588	2588	0.0	15003	15003	0	0.0
25	1196	3435	2611	2622	5.0	14970	14986	-0	63.2
49	1134	3434	2622	2644	9.5	14951	14974	-1	229.1
74	849	3432	2669	2702	13.5	14852	14949	-3	474.9
98	738	3433	2686	2731	16.6	14812	14920	-5	742.9
145	712	3437	2693	2759	22.2	14811	14885	-11	1422.1
190	697	3436	2694	2781	27.4	14811	14867	-17	2295.3
285	698	3438	2695	2826	38.4	14828	14851	-28	4907.3

D	T	S	σ_t	σ_{stp}	ΣΔD	C	C_m	K	ΣΔX
H51 continued									
377	702	3440	2696	2869	49.1	14846	14848	-38	8449.0
462	698	3439	2696	2907	59.1	14857	14848	-47	12641.1
604	636	3434	2701	2976	75.8	14956	14850	-60	21524.0
750	564	3131	2707	3050	92.4	14850	14851	-75	32777.9
943	443	3431	2721	3153	112.7	14831	14849	-95	49976.6
H52									
0	1326	3432	2583	2583	0.0	15009	15009	0	0.0
25	1178	3434	2614	2625	5.0	14963	14986	-0	63.5
50	1150	3433	2618	2641	9.7	14957	14973	-1	239.1
75	1054	3431	2634	2668	14.2	14927	14963	-2	517.7
100	876	3433	2665	2711	18.1	14865	14946	-4	859.7
149	726	3434	2688	2757	24.5	14816	14911	-9	1658.9
196	710	3437	2693	2783	30.1	14818	14889	-15	2619.8
292	699	3437	2695	2828	41.3	14830	14867	-26	5356.5
387	700	3439	2696	2873	52.4	14846	14860	-36	9134.4
479	651	3433	2698	2917	63.2	14841	14857	-46	13797.5
619	578	3429	2704	2987	79.2	14833	14852	-61	22609.4
775	507	3431	2714	3069	96.2	14830	14848	-78	34405.5
974	387	3431	2727	3175	115.8	14813	14843	-102	51563.0
1118	336	3435	2736	3249	128.6	14816	14839	-120	64998.8
H53									
0	1278	3433	2594	2594	0.0	14993	14993	0	0.0
24	1199	3433	2609	2620	4.8	14969	14981	-0	57.7
48	1114	3433	2625	2646	9.2	14944	14969	-1	218.8
72	838	3433	2671	2704	13.0	14846	14944	-3	445.3
97	729	3432	2686	2731	16.2	14809	14914	-6	716.5
140	709	3435	2692	2756	21.3	14808	14881	-11	1323.8
185	700	3437	2694	2779	26.6	14813	14864	-17	2173.0
275	702	3439	2696	2822	37.0	14828	14850	-28	4561.0
365	702	3439	2696	2862	47.4	14842	14846	-37	7912.6
444	711	3440	2695	2898	56.8	14859	14847	-45	11689.8
584	676	3436	2697	2963	73.5	14869	14851	-58	20294.2
720	588	3431	2704	3033	89.4	14855	14853	-71	30671.8
H54									
0	1194	3432	2609	2609	0.0	14964	14964	0	0.0
21	1166	3434	2616	2625	3.9	14958	14961	-1	41.8
42	1125	3433	2623	2642	7.8	14946	14956	-1	163.5
63	829	3434	2673	2702	11.1	14841	14936	-3	336.7
84	745	3434	2686	2724	13.8	14814	14908	-5	533.4
119	707	3433	2690	2745	18.0	14804	14879	-10	959.2
150	701	3436	2693	2762	21.6	14806	14864	-14	1445.8
230	697	3437	2695	2800	30.8	14819	14846	-24	3201.4
305	700	3437	2694	2834	39.6	14832	14841	-32	5537.4
382	701	3440	2697	2871	48.6	14845	14840	-41	8631.3
558	684	3438	2697	2952	69.3	14867	14845	-58	18379.9
H55									
0	1108	3433	2626	2626	0.0	14934	14934	0	0.0
18	1221	3434	2606	2614	3.3	14977	14955	-1	30.2
37	1087	3434	2630	2647	6.8	14933	14955	-1	126.9
56	1087	3435	2631	2657	10.1	14936	14948	-2	280.1
74	1066	3435	2635	2668	13.2	14932	14945	-3	481.0
140	701	3436	2693	2758	22.6	14805	14909	-9	1488.6
200	713	3435	2691	2783	29.7	14819	14880	-16	2681.8
275	701	3438	2695	2821	38.5	14827	14864	-25	4773.5
360	700	3440	2697	2861	48.3	14842	14857	-34	7907.4

D	T	S	σ_t	σ_{stp}	ΣΔD	C	C_m	K	ΣΔX
H56									
0	1066	3438	2637	2637	0.0	14920	14920	0	0.0
25	1068	3438	2637	2648	4.1	14925	14922	-1	52.0
49	999	3439	2650	2672	8.0	14904	14919	-3	195.2
74	879	3440	2670	2704	11.6	14864	14907	-5	419.6
98	766	3440	2687	2732	14.7	14824	14891	-7	684.7
148	729	3439	2692	2760	20.7	14818	14868	-13	1414.7
198	719	3440	2694	2785	26.5	14822	14855	-19	2421.2
298	707	3438	2694	2831	38.1	14833	14846	-31	5312.3
395	703	3438	2695	2875	49.6	14847	14845	-41	9279.2
H57									
0	1120	3443	2632	2632	0.0	14940	14940	0	0.0
19	1114	3444	2633	2642	3.2	14941	14940	-1	30.8
39	1006	3448	2656	2673	6.4	14906	14931	-2	123.6
58	1005	3448	2656	2682	9.2	14909	14923	-3	261.7
78	1005	3448	2656	2691	12.3	14912	14920	-4	466.0
117	996	3448	2657	2710	18.1	14915	14918	-6	1036.8
H58									
0									
11				NO FURTHER DATA COLLECTED					
34									
H59									
0	1158	3449	2629	2629	0.0	14954	14954	0	0.0
17	1162	3448	2628	2635	2.9	14958	14956	-1	25.2
35	1166	3448	2627	2643	6.1	14963	14958	-1	107.7
52	1175	3451	2628	2651	9.1	14968	14961	-1	238.5
69	1189	3460	2632	2663	12.1	14977	14963	-2	418.4
138	958	3466	2678	2740	22.6	14906	14953	-4	1503.5
186	893	3460	2684	2768	28.7	14890	14938	-8	2502.2
245	856	3457	2687	2799	36.1	14885	14926	-12	4090.7
300	815	3450	2688	2824	42.9	14878	14918	-16	5947.8
379	826	3454	2689	2862	52.7	14895	14911	-22	9277.5
440	799	3453	2693	2893	60.2	14895	14909	-27	12356.7
609	724	3445	2697	2974	80.0	14892	14905	-39	23118.3
700	694	3443	2700	3018	91.7	14894	14903	-45	30268.8
882	514	3449	2728	3131	111.1	14853	14897	-61	45607.1
H60									
0	1380	3466	2599	2599	0.0	15031	15031	0	0.0
14	1374	3466	2600	2606	2.8	15031	15031	0	19.8
28	1382	3467	2599	2611	5.6	15037	15032	1	79.4
42	1378	3466	2599	2618	8.5	15037	15034	1	179.2
56	1384	3466	2598	2623	11.3	15042	15035	1	319.6
84	1320	3469	2613	2651	16.9	15026	15035	2	708.4
162	1049	3476	2670	2743	29.8	14946	15011	1	2293.3
259	987	3473	2678	2795	43.0	14937	14985	-3	5071.0
332	930	3465	2682	2832	52.6	14928	14973	-6	7923.4
390	887	3461	2685	2862	60.2	14921	14966	-9	10646.9
488	849	3457	2688	2909	72.8	14922	14957	-14	16169.4
600	808	3452	2691	2962	87.1	14924	14951	-20	23959.7
775	689	3447	2704	3055	108.5	14906	14942	-30	38703.7
925	563	3442	2716	3138	125.3	14879	14934	-41	52951.1
H61									
0	1323	3468	2612	2612	0.0	15012	15012	0	0.0
19	1289	3468	2619	2627	3.5	15004	15008	0	33.8

D	T	S	σ_t	σ_{stp}	ΣΔD	C	C_m	K	ΣΔX
H61 continued									
38	1288	3468	2619	2636	7.0	15007	15007	0	133.7
57	1119	3471	2653	2679	10.2	14952	14998	-0	285.8
77	1118	3471	2654	2688	13.3	14955	14986	-1	490.0
93	1113	3471	2655	2697	15.7	14957	14981	-1	697.1
H62									
0	1234	3466	2628	2628	0.0	14982	14982	0	0.0
23	1236	3467	2628	2639	4.0	14986	14984	-0	46.3
46	1240	3466	2627	2647	8.0	14992	14987	-0	186.3
69	1146	3469	2647	2678	11.9	14963	14984	-1	408.3
91	1118	3469	2652	2693	15.3	14956	14978	-1	684.1
H63									
0	1189	3436	2613	2613	0.0	14963	14963	0	0.0
22	1194	3436	2612	2622	4.1	14968	14965	-1	45.9
45	1120	3438	2628	2648	8.3	14947	14961	-1	187.2
67	1073	3441	2638	2669	12.1	14934	14954	-2	398.6
90	974	3445	2659	2699	15.7	14902	14945	-3	682.5
135	887	3447	2674	2736	22.1	14878	14926	-7	1395.3
172	783	3445	2689	2767	26.8	14844	14912	-10	2117.2
253	754	3443	2691	2807	36.5	14846	14891	-18	4182.0
343	728	3441	2694	2850	47.2	14850	14879	-28	7378.2
561	695	3437	2695	2951	73.4	14871	14872	-48	19220.6
H64									
0	1160	3442	2623	2623	0.0	14953	14953	0	0.0
22	1137	3444	2629	2639	3.8	14949	14951	-1	42.8
43	1069	3446	2643	2662	7.4	14928	14945	-2	157.5
65	1045	3448	2649	2678	10.9	14925	14939	-3	346.7
87	1047	3449	2649	2689	14.3	14929	14936	-4	608.8
127	983	3446	2658	2715	20.5	15911	14931	-6	1264.2
155	886	3448	2675	2746	24.4	14881	14924	-8	1822.2
243	849	3453	2685	2796	35.8	14882	14909	-15	4089.3
337	754	3442	2691	2844	47.4	14858	14898	-23	7462.3
H65									
0	1338	3461	2603	2603	0.0	15016	15016	0	0.0
23	1300	3461	2611	2621	4.4	15007	15012	0	51.6
47	1237	3468	2629	2650	8.8	14991	15005	0	205.8
70	1125	3468	2650	2682	12.7	14956	14995	-0	428.6
94	1127	3469	2450	2693	16.4	14961	14986	-1	735.4
H66									
0	1517	3436	2546	2546	0.0	15071	15071	0	0.0
15	1472	3449	2566	2573	3.6	15062	15067	1	27.4
29	1451	3451	2572	2585	6.9	15057	15063	1	98.7
44	1427	3454	2579	2599	10.2	15053	15060	2	222.4
H67									
0	1406	3458	2587	2587	0.0	15038	15038	0	0.0
10	1401	3458	2588	2592	2.1	15038	15038	0	10.6
20	1402	3459	2589	2597	4.2	15040	15039	1	42.6
29	1398	3459	2589	2602	6.1	15041	15039	1	89.5
49	1375	3462	2596	2618	10.3	15037	15039	1	252.9
H68									
0	1354	3459	2598	2598	0.0	15022	15022	0	0.0
10	1353	3459	2599	2603	2.0	15023	15022	0	10.1

D	T	S	σ_t	σ_{stp}	ΣΔD	C	C_m	K	ΣΔX
H68 continued									
24	1345	3461	2602	2613	4.8	15022	15022	0	58.1
39	1340	3461	2603	2620	7.8	15024	15022	1	152.7
H69									
0	1473	3429	2550	2550	0.0	15057	15057	0	0.0
10	1469	3429	2551	2556	2.4	15057	15057	0	12.4
20	1471	3429	2551	2560	4.9	15059	15057	1	49.7
30	1469	3430	2552	2565	7.4	15060	15058	1	111.8
40	1476	3429	2550	2567	9.9	15064	15059	2	199.1
H70									
0	1534	3351	2477	2477	0.0	15066	15066	0	0.0
10	1526	3358	2484	2489	3.1	15066	15066	0	15.7
20	1509	3388	2511	2520	6.1	15066	15066	1	60.6
30	1497	3401	2524	2537	8.9	15066	15066	1	130.9
35	1499	3412	2532	2547	10.3	15069	15066	2	175.0
H71									
0	1507	3437	2549	2549	0.0	15068	15068	0	0.0
10	1495	3437	2552	2556	2.4	15066	15067	0	12.4
20	1500	3437	2551	2559	4.9	15069	15067	1	49.7
30	1497	3438	2552	2565	7.4	15070	15068	1	111.8
35	1500	3439	2552	2568	8.7	15073	15069	2	152.2
H72									
0	1468	3451	2568	2568	0.0	15058	15058	0	0.0
17	1465	3451	2569	2577	3.9	15060	15059	1	33.4
35	1447	3454	2575	2591	8.0	15058	15059	1	140.6
52	1420	3456	2582	2606	11.8	15051	15057	2	305.5
69	1367	3463	2599	2630	15.4	15037	15054	2	523.7
86	1292	3466	2616	2655	18.7	15016	15049	3	782.5
104	1244	3469	2628	2675	22.0	15003	15042	3	1095.3
H73									
0	1416	3456	2583	2583	0.0	15041	15041	0	0.0
24	1416	3456	2583	2594	5.2	15045	15043	1	62.7
48	1407	3458	2587	2608	10.4	15047	15044	1	250.1
72	1363	3460	2597	2630	15.4	15036	15043	2	553.7
97	1364	3460	2597	2641	20.6	15041	15042	3	990.0
137	1248	3467	2626	2687	28.4	15009	15037	3	1896.9
H74									
0	1381	3468	2600	2600	0.0	15032	15032	0	0.0
20	1381	3468	2600	2609	4.0	15035	15033	0	40.4
40	1381	3468	2600	2618	8.0	15038	15035	1	161.9
58	1380	3468	2600	2626	11.7	15041	15036	1	341.0
75	1333	3470	2611	2645	15.1	15029	15036	2	564.9
107	1215	3480	2642	2690	20.8	14995	15029	2	1084.7
130	1148	3483	2657	2716	24.4	14975	15021	2	1513.1
189	1052	3482	2674	2759	32.8	14951	15003	0	2858.8
251	971	3473	2681	2795	41.1	14931	14987	-2	4672.7
333	901	3464	2685	2836	51.6	14917	14972	-6	7758.7
465	835	3458	2691	2902	68.3	14912	14955	-14	14395.7
600	791	3453	2694	2966	85.1	14917	14946	-21	23343.5
765	688	3445	2702	3050	105.1	14903	14938	-31	37019.6
826	628	3445	2710	3086	112.16	14889	14935	-36	42589.2

D	T	S	σ_t	σ_{stp}	ΣΔD	C	C_m	K	ΣΔX
H75									
0	1396	3468	2597	2597	0.0	15036	15036	0	0.0
23	1384	3468	2599	2609	4.6	15036	15036	1	53.9
46	1268	3472	2626	2647	9.0	15002	15028	1	205.1
69	1185	3477	2646	2677	12.9	14978	15015	1	428.7
91	1129	3481	2659	2700	16.3	14962	15004	0	699.1
135	1054	3478	2671	2732	22.6	14943	14987	-1	1408.0
180	1033	3480	2676	2757	28.7	14942	14976	-3	2370.0
265	967	3473	2682	2802	39.9	14931	14963	-6	4863.3
367	877	3462	2688	2854	52.9	14913	14952	-12	8987.1
585	815	3466	2700	2965	79.5	14926	14940	-24	21647.9
H76									
0	1474	3470	2582	2582	0.0	15062	15062	0	0.0
20	1467	3469	2582	2591	4.3	15063	15062	1	43.7
39	1449	3467	2585	2602	8.5	15060	15062	2	166.0
59	1318	3469	2614	2640	12.6	15020	15054	2	365.7
79	1166	3468	2642	2678	16.1	14972	15040	2	609.7
118	1008	3475	2676	2730	21.8	14923	15009	1	1176.6
158	957	3471	2682	2753	27.0	14910	14985	-2	1892.0
225	894	3465	2687	2790	35.4	14897	14961	-6	3500.3
280	867	3460	2688	2815	42.2	14896	14948	-10	5217.7
341	846	3457	2689	2844	49.8	14897	14939	-14	7569.5
451	830	3457	2691	2896	63.5	14909	14930	-21	12982.2
550	797	3455	2695	2944	75.7	14912	14926	-27	19100.7
684	720	3448	2700	3011	91.9	14903	14923	-35	29105.9
852	584	3441	2713	3101	111.0	14876	14916	-48	43797.3
1367	326	3449	2748	3374	158.9	14856	14897	-94	96878.5
1703	262	3460	2762	3541	182.9	14885	14892	-123	133804.6
H77									
0	1352	3462	2601	2601	0.0	15021	15021	0	0.0
16	1342	3463	2604	2611	3.1	15021	15021	0	25.5
47	1314	3464	2610	2632	9.2	15017	15019	1	215.6
62	1300	3465	2614	2642	12.1	15014	15018	1	372.1
93	1133	3467	2648	2690	17.5	14963	15009	1	790.6
165	928	3467	2683	2758	27.7	14900	14975	-3	2111.3
264	868	3459	2687	2807	40.1	14893	14945	-10	4770.5
351	830	3456	2690	2850	50.9	14892	14932	-16	8079.9
405	809	3455	2693	2877	57.5	14892	14927	-20	10573.8
502	770	3451	2695	2924	69.2	14893	14920	-27	15901.2
686	690	3445	2702	3014	91.1	14891	14913	-40	28899.8
835	579	3442	2714	3095	107.8	14871	14907	-52	41584.2
1499	290	3452	2753	3440	167.3	14862	14889	-111	111025.2
H78									
0	1404	3464	2592	2592	0.0	15039	15039	0	0.0
23	1358	3459	2598	2608	4.7	15026	15032	0	54.7
47	1282	3467	2619	2640	9.4	15006	15024	1	218.1
70	1258	3463	2621	2652	13.6	15001	15017	1	465.8
94	1049	3470	2665	2708	17.5	14934	15005	0	786.0
141	933	3466	2682	2746	23.8	14897	14975	-2	1528.0
180	914	3466	2685	2767	28.7	14897	14958	-5	2315.5
261	863	3460	2688	2807	38.8	14891	14938	-11	4527.9
341	838	3456	2689	2844	48.6	14894	14927	-17	7499.8
547	788	3453	2694	2942	74.1	14908	14917	-30	18780.2
670	731	3448	2699	3003	89.0	14905	14915	-38	27890.0
842	616	3442	2710	3093	109.0	14887	14911	-50	43009.7

D	T	S	σ_t	σ_{stp}	ΣΔD	C	C_m	K	ΣΔX
H78 continued									
1046	427	3438	2729	3208	130.0	14843	14902	-68	62783.1
1276	348	3445	2742	3327	150.1	14848	14892	-92	86172.4
1706	261	3461	2763	3543	181.7	14885	14886	-130	133219.6
2132	227	3469	2772	3742	208.5	14944	14891	-154	184615.0
H79									
0	1535	3441	2546	2546	0.0	15078	15078	0	0.0
24	1428	3467	2589	2600	5.5	15050	15064	1	67.0
48	1356	3477	2612	2633	10.4	15032	15052	2	241.6
72	1211	3482	2645	2677	14.6	14987	15038	2	495.4
97	1123	3484	2663	2707	18.4	14962	15022	1	817.8
145	1077	3484	2671	2737	25.2	14953	15000	0	1636.1
193	1044	3483	2676	2763	31.7	14949	14988	-2	2735.9
286	970	3475	2683	2812	43.9	14936	14973	-5	5666.1
380	919	3468	2686	2858	56.1	14932	14964	-9	9702.1
473	865	3462	2690	2904	67.9	14926	14957	-14	14756.6
620	789	3454	2695	2976	86.3	14920	14949	-21	24806.2
765	688	3447	2704	3051	103.8	14904	14942	-30	36894.1
H80									
0	1586	3433	2528	2528	0.0	15193	15093	0	0.0
23	1561	3438	2538	2548	6.1	15089	15091	1	70.2
46	1398	3469	2597	2618	11.4	15045	15079	2	255.5
69	1248	3474	2631	2662	15.8	14999	15060	3	506.3
91	1236	3475	2634	2675	19.6	14998	15045	3	809.8
137	1203	3479	2644	2705	27.3	14995	15029	3	1687.2
155	1176	3482	2651	2721	30.2	14990	15025	3	2107.9
H81									
0	1539	3428	2535	2535	0.0	15077	15077	0	0.0
19	1515	3440	2550	2558	4.8	15074	15076	1	46.3
39	1388	3467	2598	2615	9.4	15040	15066	2	178.2
58	1275	3482	2632	2658	13.0	15008	15052	2	352.2
78	1168	3488	2658	2693	16.2	14975	15037	2	570.8
117	1155	3500	2669	2722	21.8	14978	15017	1	1117.5
155	1157	3500	2669	2739	27.1	14985	15008	1	1837.7
H82									
0	1600	3435	2527	2527	0.0	15097	15097	0	0.0
16	1564	3452	2548	2555	4.1	15091	15094	1	33.4
31	1343	3484	2620	2634	7.4	15026	15077	2	110.1
47	1186	3492	2657	2678	10.1	14977	15051	2	213.6
63	1170	3491	2659	2688	12.4	14973	15032	1	343.4
95	1166	3495	2663	2706	17.1	14978	15013	1	710.6
125	1132	3491	2667	2723	21.3	14971	15003	0	1181.2
184	1100	3487	2669	2752	29.6	14968	14993	-1	2464.7
243	1054	3484	2675	2785	37.8	14961	14986	-2	4203.4
323	983	3475	2681	2826	48.5	14947	14978	-5	7240.5
415	908	3466	2686	2874	60.5	14933	15969	-8	11677.4
550	835	3459	2692	2941	77.7	14927	14960	-15	19969.6
716	731	3449	2699	3024	98.2	14913	14950	-24	32917.7
858	621	3445	2711	3101	114.6	14893	14942	-33	45853.9
H83									
0	1491	3453	2565	2565	0.0	15065	15065	0	0.0
20	1489	3453	2565	2574	4.7	15068	15067	1	47.0
39	1449	3459	2579	2596	9.0	15059	15065	2	175.4
59	1195	3487	2652	2678	12.8	14981	15050	2	360.2

D	T	S	σ_t	σ_{stp}	ΣΔD	C	C_m	K	ΣΔX
H83 continued									
79	1152	3490	2662	2698	15.8	14969	15031	2	566.3
120	1117	3488	2667	2721	21.6	14963	15009	1	1148.5
208	1066	3486	2675	2769	33.8	14959	14989	-2	3143.5
282	1012	3480	2679	2807	43.7	14952	14980	-4	5574.8
449	872	3461	2688	2891	65.4	14925	14964	-11	13519.9
535	807	3455	2693	2936	76.3	14914	14957	-15	18844.6
647	758	3451	2697	2991	90.0	14912	14950	-22	26982.1
829	633	3446	2710	3087	111.2	14893	14939	-34	42629.4
1028	478	3443	2727	3197	131.8	14862	14927	-50	61747.9
1651	278	3460	2761	3516	182.6	14884	14907	-103	129743.6
H84									
0	1512	3454	2561	2561	0.0	15072	15072	0	0.0
19	1502	3454	2563	2572	4.5	15072	15072	1	42.9
38	1187	3490	2656	2673	8.1	14975	15048	1	147.7
57	1156	3493	2664	2689	10.9	14968	15022	1	279.6
115	1127	3493	2669	2721	19.1	14967	14995	-0	981.3
140	1098	3491	2673	2736	22.5	14960	14989	-1	1419.0
206	1052	3484	2676	2769	31.4	14954	14979	-3	2962.9
277	998	3478	2680	2806	40.9	14945	14971	-5	5245.6
335	948	3472	2684	2836	48.5	14935	14966	-8	7559.9
437	866	3461	2689	2887	61.5	14921	14957	-12	12593.1
505	823	3457	2692	2921	70.0	14915	14952	-16	16609.3
602	791	3454	2695	2967	82.0	14917	14946	-22	23266.7
764	686	3448	2705	3052	101.5	14903	14939	-31	36523.2
H85									
0	1548	3443	2545	2545	0.0	15082	15082	0	0.0
20	1546	3444	2546	2555	5.0	15085	15083	1	50.7
39	1281	3443	2601	2618	9.4	15002	15064	2	178.4
59	1202	3498	2659	2685	12.8	14985	15040	2	349.4
178	1093	3491	2674	2754	29.7	14965	14996	-0	2345.4
219	1036	3485	2679	2778	35.2	14950	14989	-2	3433.2
303	972	3475	2682	2819	46.2	14940	14977	-5	6301.0
405	894	3465	2687	2871	59.3	14926	14966	-9	10947.9
515	840	3459	2691	2924	73.2	14924	14957	-15	17346.1
655	771	3452	2696	2993	90.6	14919	14949	-22	27540.2
785	664	3447	2707	3064	106.0	14897	14942	-30	38640.8
984	509	3443	2723	3173	127.2	14867	14930	-46	57393.7
1385	329	3449	2747	3381	162.8	14859	14911	-83	99470.8
1637	276	3462	2763	3511	180.8	14880	14904	-105	126715.1
H86									
0	1591	3441	2533	2533	0.0	15095	15095	0	0.0
22	1571	3450	2545	2555	5.7	14093	15094	1	62.8
45	1306	3475	2621	2641	10.7	15016	15074	2	231.6
67	1195	3491	2655	2685	14.4	14983	15049	2	437.6
89	1180	3496	2661	2702	17.6	14982	15033	2	692.2
134	1131	3491	2667	2727	24.1	14972	15014	1	1412.0
178	1098	3489	2671	2752	30.3	14966	15003	0	2371.9
263	1043	3483	2676	2795	41.9	14960	14990	-2	4934.1
355	950	3471	2683	2843	54.1	14939	14980	-5	8713.5
435	891	3463	2686	2883	64.5	14929	14971	-8	12815.6
572	817	3455	2692	2951	82.0	14923	14960	-15	21618.7
712	747	3449	2697	3020	99.4	14919	14952	-23	32828.2
894	594	3442	2712	3119	120.6	14887	14942	-34	49853.4
1113	454	3446	2732	3240	142.7	14867	14929	-52	72021.8
1347	350	3449	2745	3362	162.8	14961	14918	-74	96762.9
1828	258	3463	2765	3599	197.7	14905	14909	-111	152085.1

A. R. SHEARER, GOVERNMENT PRINTER
WELLINGTON, NEW ZEALAND—1975